



The Journal of The Royal Astronomical Society of Canada
Journal
Le Journal de la Société royale d'astronomie du Canada

PROMOTING
ASTRONOMY
IN CANADA

February/février 2020
Volume/volume 114
Number/numéro 1 [800]

Inside this issue:

The Pioneer Anomaly

**Playing with
Magnitudes**

**Atmospheric Display
of a Lifetime!**

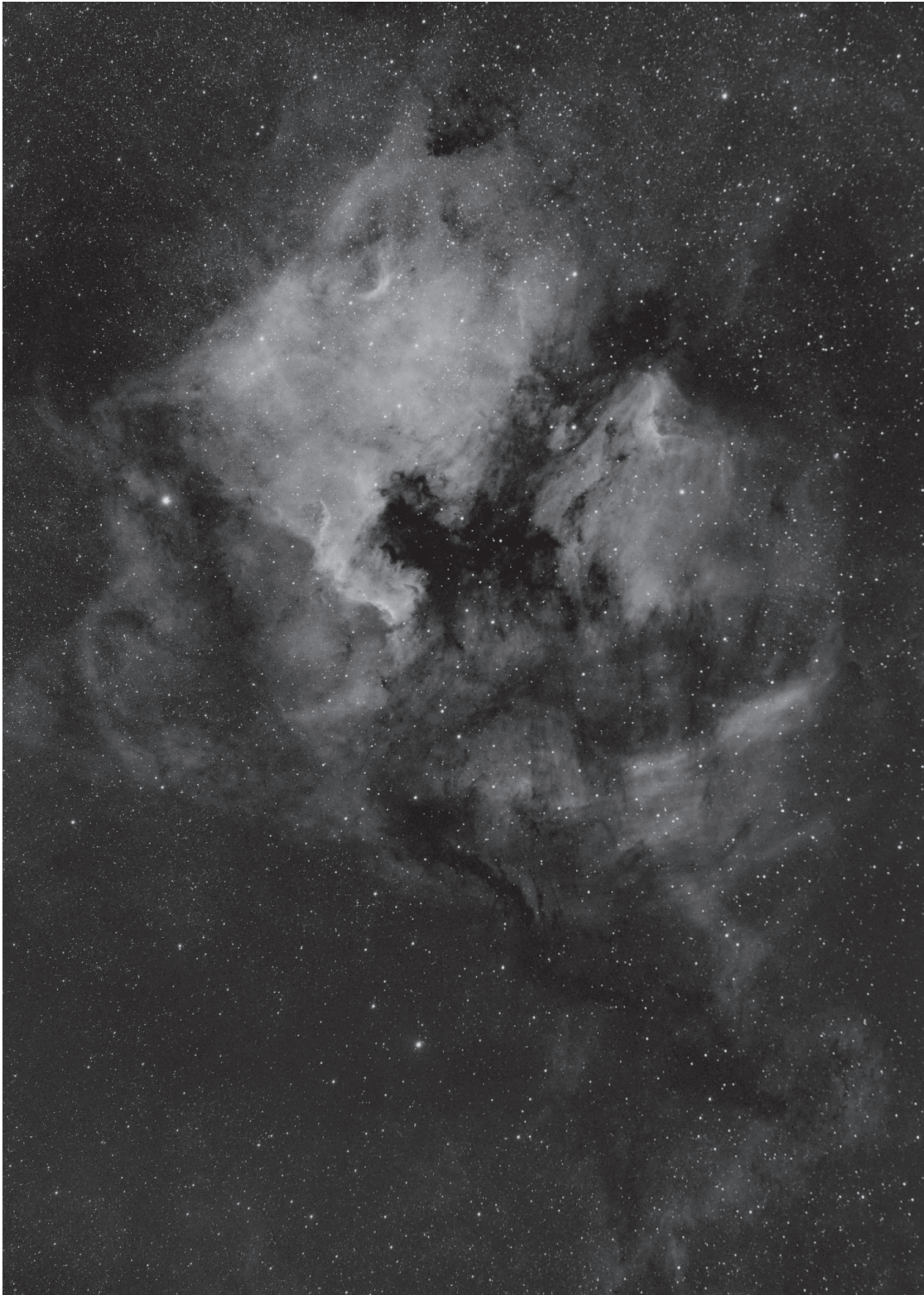
**Sidney Girling and
Joseph Pearce**

**Stellar Space-Density
Analyses**

The Charioteer

The Best of Monochrome.

Drawings, images in black and white, or narrow-band photography.



The North America and Pelican region of Cygnus was imaged by Godfrey Booth. He used a ZWO 1600 cooled camera on a Celestron CGEM mount. The image was processed with PixInsight. The final is about 90 minutes' worth of H α data.

contents / table des matières

Feature Articles / Articles de fond

- 7 **The Pioneer Anomaly as a Coulomb Attraction**
by Steven L. Morris
- 9 **Playing with Magnitudes**
by Gunter Hoering
- 10 **Atmospheric Display of a Lifetime!**
by Rick Stankiewicz
- 12 **Sidney Girling and Joseph Pearce at the Dominion Astrophysical Observatory**
by Donald C. Morton
- 16 **Methods of Stellar Space-Density Analyses: A Retrospective Review**
by B. Cameron Reed
- 24 **Pen and Pixel: Northern lights / Moon / M45 / NGC733**
by Allendria Brunjes / Klaus Brasch / Debra Ceravolo / Blair MacDonald

Columns / Rubriques

- 28 **Skyward: A Daydream and Poetry among the Stars**
by David Levy
- 31 **Observing: A Simple Small 'Scope**
by Chris Beckett

- 33 **Binary Universe: Charts of the Sky**
by Blake Nancarrow
- 38 **CFHT Chronicles: Welcome 2020!**
by Mary Beth Laychak
- 41 **Dish on the Cosmos: Chasing the Origins of Galactic Magnetic Fields**
by Erik Rosolowsky
- 43 **John Percy's Universe: The Scale of the Universe**
by John R. Percy
- 46 **Celestial Review: Celestial Events for 2020**
by Dave Garner

Departments / Départements

- 2 **President's Corner**
by Dr. Chris Gainor
- 3 **News Notes / En manchettes**
Compiled by Jay Anderson
- 27 **Great Images**
by Michael Gatto
- 48 **Astrocryptic and December Answers**
by Curt Nason
- iii **Great Images**
by Nicole Laporte

Ron Brecher imaged the nebulosity around Auriga, the Charioteer from his SkyShed in Guelph, Ontario. Ron used a Takahashi FSQ-106 ED IV @ f/3.6, QHY367C one-shot colour camera, and Optolong L-eNhance narrowband filter, on a Paramount MX, unguided. All pre-processing and processing was done in PixInsight.



Journal

The *Journal* is a bi-monthly publication of The Royal Astronomical Society of Canada and is devoted to the advancement of astronomy and allied sciences. It contains articles on Canadian astronomers and current activities of the RASC and its Centres, research and review papers by professional and amateur astronomers, and articles of a historical, biographical, or educational nature of general interest to the astronomical community. All contributions are welcome, but the editors reserve the right to edit material prior to publication. Research papers are reviewed prior to publication, and professional astronomers with institutional affiliations are asked to pay publication charges of \$100 per page. Such charges are waived for RASC members who do not have access to professional funds as well as for solicited articles. Manuscripts and other submitted material may be in English or French, and should be sent to the Editor-in-Chief.

Editor-in-Chief

Nicole Mortillaro
Email: editor@rasc.ca
Web site: www.rasc.ca
Telephone: 416-924-7973
Fax: 416-924-2911

Associate Editor, Research

Douglas Hube
Email: dhube@ualberta.ca

Associate Editor, General

Michael Attas
Email: attasm1@mymts.net

Assistant Editors

Michael Allen
Martin Beech
Dave Chapman
Ralph Chou
Ralph Croning
Dave Garner
Patrick Kelly

Production Manager

James Edgar
Email: james@jamesedgar.ca

Contributing Editors

Jay Anderson (News Notes)
Chris Beckett (Observing Tips)
Mary Beth Laychak (CFHT Chronicles)

Her Excellency the Right Honourable **Julie Payette**, C.C., C.M.M., C.O.M., C.Q., C.D., Governor General of Canada, is the Viceregal Patron of the RASC.

The *Journal* of The Royal Astronomical Society of Canada is published at an annual subscription rate of \$93.45 (including tax) by The Royal Astronomical Society of Canada. Membership, which includes the publications (for personal use), is open to anyone interested in astronomy. Applications for subscriptions to the *Journal* or membership in the RASC and information on how to acquire back issues of the *Journal* can be obtained from:

The Royal Astronomical Society of Canada
203 – 4920 Dundas St W
Toronto ON M9A 1B7, Canada

Email: nationaloffice@rasc.ca
Web site: www.rasc.ca
Telephone: 416-924-7973
Fax: 416-924-2911

Canadian Publications Mail Registration No. 09818
Canada Post: Send address changes to 203 – 4920 Dundas St W, Toronto ON M9A 1B7

Canada Post Publication Agreement No. 40069313

We acknowledge the financial support of the Government of Canada through the Canada Periodical Fund (CPF) for our publishing activities.

© 2020 The Royal Astronomical Society of Canada.
All rights reserved. ISSN 0035-872X

Canada



President's Corner

by Christopher Gainor, Ph.D., Victoria Centre
(cgainor@shaw.ca)

In the December issue of the *Journal*, I gave up this space to my friend Randy Attwood, who shared his thoughts as he wrapped up five memorable years as Executive Director of The Royal Astronomical Society of Canada.

When Randy retired in October, I was proud to acknowledge the many contributions he has made to the RASC during his half century as a member, capped by his time as ED. He has served in many capacities, including as President of the Toronto and Mississauga Centres and as the National President who brought the RASC into the 21st century.

Randy played a key role in transforming the RASC during his time as ED, including purchasing *SkyNews*, bringing forward the robotic telescope, and most importantly expanding our fundraising, something that is already benefitting the Society and its members.

I can't think of anyone who has done more for the RASC in recent decades than Randy Attwood. I know that he and his wonderful wife Betty Robinson will remain involved in the Society, and we will be counting on their wisdom and assistance in the days (and nights) to come.

As many of you know, the Board of Directors chose Philip Groff of Toronto to succeed Randy as ED. Although Phil is new to the RASC, he brings great experience running organizations, along with knowledge obtained through his academic specialty of psychology. I'm pleased to say that we already have Phil out observing.

The RASC at the national level is bigger and more complex today than it was a few years ago. We will be counting on Phil to make sure that the Society and its governance structures are updated so that we can better meet the challenges of serving our members and promoting astronomy around Canada. He is working with the Board to reimagine and restructure our committees to make them more effective.

On Randy's watch, we made use of grants and charitable contributions to bring in new staff and new services, and Phil has been charged with updating our human resources policies and practices.

We are continuing to work on bringing our online infrastructure up to date. Today that infrastructure is fragmented and requires major changes to make it more useful in our increasingly complicated online world. We need to deal with the problems some members have encountered with our website and with our email lists.

Last year I worked with both Randy and Phil to deal with major financial and human resources challenges at *SkyNews*. Now we are moving forward there with a new managing editor and fresh contributors. We have formed a new editorial board to help improve all our publications, including the *Journal*.

We all recognize the vital importance of our Centres, and Phil is making an effort to visit every Centre as soon as he can. We on the Board are working with Phil and with National

Council to strengthen our bonds with the Centres and to make sure that the Society is doing everything it can to help the Centres do a better job of serving their members and reaching out to their communities.

We are always happy to hear from members about what the Society is doing right and what we can do better. Don't hesitate to reach out to Phil or me or any of my colleagues on the Board of Directors. ★

News Notes / En manchette

(Compiled by Jay Anderson)

What makes a black hole shine?

For decades, scientists have speculated about the origin of the electromagnetic radiation emitted from celestial regions that host black holes and neutron stars—the most mysterious objects in the Universe. Astrophysicists believe that this high-energy radiation—which makes neutron stars and black holes shine bright—is generated by electrons that move at nearly the speed of light, but the process that accelerates these particles has remained a mystery.

Now, two researchers at Columbia University have presented a new explanation for the physics underlying the acceleration of these energetic particles.

Astrophysicists Luca Comisso and Lorenzo Sironi employed massive super-computer simulations to calculate the

mechanisms that accelerate these particles. They concluded that their energization is a result of the interaction between chaotic motion and reconnection of super-strong magnetic fields.

“Turbulence and magnetic reconnection—a process in which magnetic field lines tear and rapidly reconnect—conspire together to accelerate particles, boosting them to velocities that approach the speed of light,” said Comisso, a postdoctoral research scientist at Columbia and first author on the study.

“The region that hosts black holes and neutron stars is permeated by an extremely hot gas of charged particles, and the magnetic field lines dragged by the chaotic motions of the gas drive vigorous magnetic reconnection,” he added. “It is thanks to the electric field induced by reconnection and turbulence that particles are accelerated to the most extreme energies, much higher than in the most powerful accelerators on Earth, like the Large Hadron Collider at CERN.”

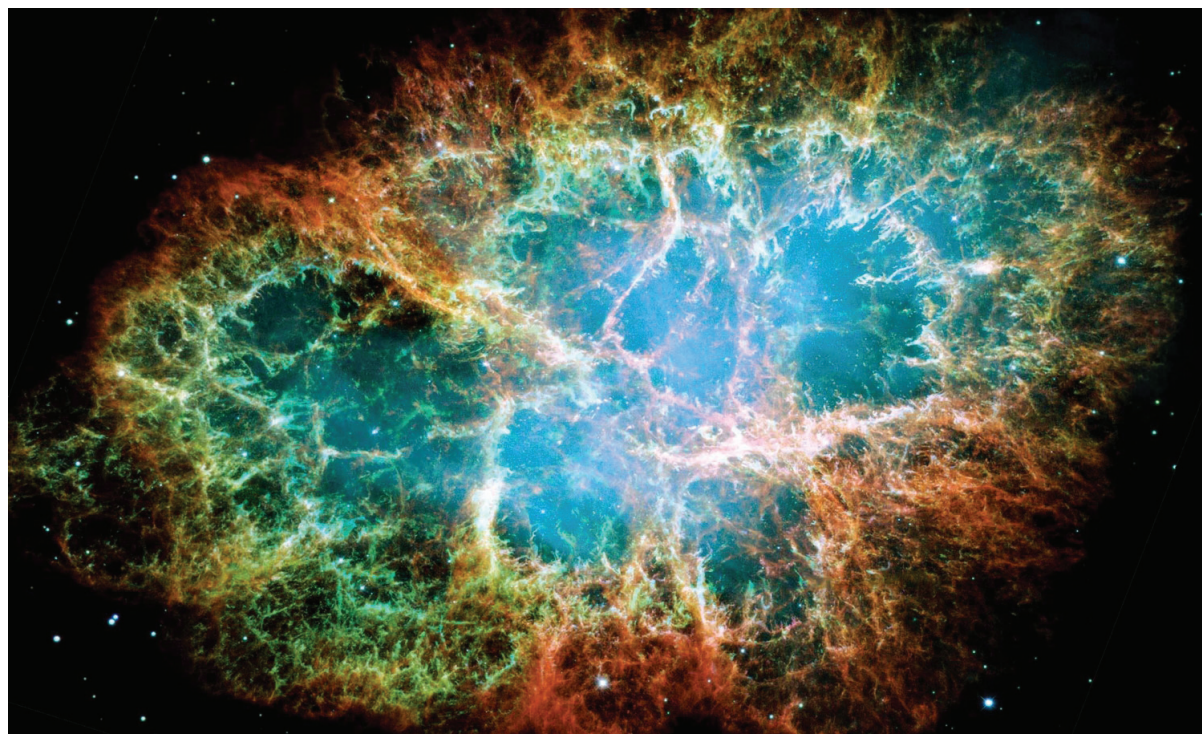


Figure 1 — A Hubble Space Telescope image of the Crab Nebula. The radiation emitted by the neutron star at the centre of the nebula is thought to be a consequence of plasma reconnection and turbulence. Image: NASA, ESA, Hubble, J. Hester, A. Loll (ASU)

Reconnection is the breaking and fusion of oppositely directed magnetic fields in a plasma. In the process, the magnetic energy is transformed into thermal and kinetic energy, accelerating electrons and other charged particles to extremely high velocities. Reconnection is responsible, at least in part, for the generation of solar flares and the creation of aurorae.

When studying turbulent gas, scientists cannot predict chaotic motion precisely. Dealing with the mathematics of turbulence is difficult, and it constitutes one of the seven “Millennium Prize” mathematical problems. To tackle this challenge from an astrophysical point of view, Comisso and Sironi designed extensive super-computer simulations—among the world’s largest ever done in this research area—to solve the equations that describe the turbulence in a gas of charged particles.

“We used the most precise technique for calculating the trajectories of hundreds of billions of charged particles that self-consistently dictate the electromagnetic fields. And it is this electromagnetic field that tells them how to move,” said Sironi, assistant professor of astronomy at Columbia and the study’s principal investigator. Sironi said that the crucial point of the study was to identifying the role magnetic reconnection plays within the turbulent environment. The simulations showed that reconnection is the key mechanism that selects the particles that will be subsequently accelerated by the turbulent magnetic fields up to the highest energies.

The simulations also revealed that particles gained most of their energy by bouncing randomly at an extremely high speed off the turbulence fluctuations. When the magnetic field is strong, this acceleration mechanism is very rapid. But the strong fields also force the particles to travel in a curved path, and by doing so, they emit electromagnetic radiation.

“This is indeed the radiation emitted around black holes and neutron stars that make them shine, a phenomenon we can observe on Earth,” Sironi said.

They plan to connect their work even more firmly with observations by comparing their predictions with the electromagnetic spectrum emitted from the Crab Nebula, the most intensely studied bright remnant of a supernova (a star that violently exploded in the year 1054). This will be a stringent test for their theoretical explanation.

Compiled with material provided by Columbia University

Dark energy goes dark?

It is a tenet of modern cosmology that the rate of expansion of the Universe is increasing, pushed by a mysterious “dark energy.” This cosmological growth was detected in studies of distant Type Ia supernovae, whose luminosity and redshift values did not fit a steady expansion of the Universe, but instead reflected an acceleration that is pushing objects away

from each other at an increasing rate. The 2011 Nobel Prize was awarded for this discovery.

In 2015, Oxford University professor Subir Sakar and colleagues published a paper claiming that the Type Ia dataset contained errors in adjustments used to account for interstellar dust and for differences between individual supernovae. In December 2019, he and his colleagues, Jacques Colin and Roya Mohayaee (Institut d’Astrophysique, Paris) and Mohamed Rameez (Niels Bohr Institute, Copenhagen), followed up on this hypothesis by publishing a new study that reinforced their earlier point of view.

Galaxies have both a cosmological velocity dictated by the expansion of the Universe and a local velocity that reflects their orbital motion within galaxy clusters and other large-scale structures. For Earth, this is a velocity of 600 km/s with respect to the cosmic microwave background (CMB). Measurements of redshift contain both of these influences, and so to determine the cosmological velocity, the local velocity must be removed. One way to do this is to avoid using measurements from nearby objects but instead only to study the distant ones, where cosmological velocities swamp the much smaller local velocities. This division is normally taken to be around 500 million light-years, but Sakar’s analysis of 740 supernovae shows that these local movements go out at least twice that far, corrupting the data used to measure the expansion of the Universe.

The researchers removed all of the corrections made to the original redshift and magnitude calculations that had been applied to correct for local motions and then examined the measurements to see if the acceleration of the Universe was equal in all directions. Their results revealed a “dipole” in the distribution of radial velocities aligned with the direction of the Earth’s motion. No significant acceleration component associated with the CMB was found. This suggested that the data used to determine the increasing expansion rate of the Universe was “fooled” by the underlying local motions.

“The supernova data indicate, with a statistical significance of 3.9σ , a dipole anisotropy in the inferred acceleration in the same direction as we are moving locally, which is indicated by a similar, well-known, dipole in the CMB,” says Sarkar. “By contrast any isotropic (monopole) acceleration which can be ascribed to dark energy is 50 times smaller and consistent with being zero at 1.4σ .”

“If you look at supernovae in only a small part of the sky, it would look like you had cosmic acceleration,” he continues. “But we are saying that it is just a local effect, that we are non-Copernican observers. It has nothing to do with the overall dynamics of the Universe and therefore nothing to do with dark energy.”

Adam Reiss, one of the Nobel Prize recipients for the original work, disputes the analysis as using an outdated and smaller

supernovae sample and for ignoring other evidence for acceleration. “The evidence for cosmic acceleration and dark energy are much broader than only the supernovae Ia sample, and any scientific case against cosmic acceleration needs to take those into account,” he says.

Compiled with material provided by Oxford University.

Interstellar comet “just passing through”

On August 30 last year, Crimean amateur astronomer Gennady Borisov discovered a comet, now identified as an interstellar visitor, passing through the Solar System on its way back into deep space. Comet Borisov has now passed its closest point to the Earth and is headed out of the Solar System, but not before attracting enormous attention because of its foreign origin.

Retrospective searches for the comet using historical images from the Catalina Sky Survey identified Borisov as far back as December 2018. Its appearance so far back, at eight times the distance of the Sun from Earth, suggests outgassing of a volatile molecule such as CO or CO₂ rather than water vapour.

Yale astronomers Pieter van Dokkum, Cheng-Han Hsieh, Shany Danieli, and Gregory Laughlin captured an image on November 24 using the W.M. Keck Observatory’s Low-Resolution Imaging Spectrometer in Hawaii. According to van Dokkum, the comet’s tail was nearly 160,000 km long. “It’s humbling to realize how small Earth is next to this visitor from another solar system,” van Dokkum said.

Laughlin noted that 2I/Borisov is evaporating as it gets closer to Earth, releasing gas and fine dust in its tail. “Astronomers are taking advantage of Borisov’s visit, using telescopes such as Keck to obtain information about the building blocks of planets in systems other than our own,” Laughlin said.

Comet Borisov has been estimated to have a nucleus between 2 and 16 km in size with the consensus opinion falling at the lower end of the range. Its composition is not unusual, being similar to Solar System comets with cyanogen and diatomic carbon prominent in the spectrum, though its low carbon abundance suggests a character similar to Jupiter-system comets that originated in the Kuiper Belt. In September, David Lewitt and Jane Luu estimated that the comet was losing water at a rate of 60 kg/s and expelling dust at a rate of 2 kg/s. Borisov was expected to peak at a magnitude of about 15 around the New Year.

The detection of Borisov and the earlier fuss about ‘Oumuamua suggests that extra-Solar System objects are fairly common—perhaps as many as a dozen at any one time in the Solar System.

Compiled with material provided by NASA



Figure 2 — The Hubble Space Telescope photographed comet 2I/Borisov at a distance of 418 million kilometres from Earth on 2019 October 12. The image reveals a central concentration of dust around the nucleus (which is too small to be seen by Hubble). The comet is falling toward the Sun and will make its closest approach on 2019 December 7, when it will be twice as far from the Sun as Earth. The comet is following a hyperbolic path around the Sun and will exit back into interstellar space. Image: NASA, ESA and D. Jewitt (UCLA)

A window to the Big Bang

In the immediate aftermath of the Big Bang, the Universe coalesced into a hot soup of elementary particles caught up in a rapidly expanding physical frame. Temperatures were so high that random motions within the particle soup reached relativistic speeds and the constituents were involved in continuous particle-antiparticle creation and destruction. After about a millionth of a second, the Universe cooled sufficiently that protons and neutrons could form and at the one-second mark, electrons and positrons. A few minutes later, some protons and neutrons combined to form deuterium, helium, and lithium.

In these early moments, the newly created nuclei were totally ionized, immersed in a sea of high-speed electrons. The electrons were very good at scattering photons (which were the dominant component at the time) and so the Universe was opaque. This state lasted for about 100,000 years, at which point things had cooled enough for the electrons and nuclei to combine into neutral (mostly hydrogen) atoms. As this recombination progressed, the Universe became transparent; the photons became the remnant cosmic microwave background (CMB) that we see today. The Universe was dark, mostly because there were no light sources other than the CMB. That situation changed when stars—or something—began to form and radiate ultraviolet energy to re-ionize the hydrogen and other nuclei. Free electrons appeared again, but the density of the Universe was now so low that the opaque plasma soup of earlier epochs was no longer possible.



Figure 3 — This image, taken with the NASA/ESA Hubble Space Telescope, shows a massive galaxy cluster, about 4.6 billion light-years away. Along its borders four bright arcs are visible; these are copies of the same distant galaxy, nicknamed the Sunburst Arc. The Arc is a galaxy almost 11 billion light-years away and the light from it is being lensed into multiple images by gravitational lensing. The Sunburst Arc is among the brightest lensed galaxies known and its image is visible at least 12 times within the four arcs. Three arcs are visible in the top right of the image, the fourth arc in the lower left. The last one is partially obscured by a bright foreground star, which is located in the Milky Way. Inset: Visible and infrared light shine from a single star-forming region in the Sunburst Arc galaxy (centre). The spot of light is duplicated six times in the arc. Image: ESA/Hubble, NASA, Rivera-Thorsen et al.

Just where all this energy came from is a puzzle for astronomers. When the massive stars that produce ionizing radiation are born, they are typically immersed in a dense thicket of dust and gas that traps outgoing radiation within the host galaxy. It would seem that not enough radiation escapes from galaxy confinement to ionize the intergalactic medium. And yet, escape it must, given the ionization of the cosmic inventory of hydrogen. Looking for that ionizing radiation is not possible, as intervening dust and gas clouds absorb the radiation long before it can reach us. Instead, astronomers must settle for a closer proxy that can stand in for earlier galaxies.

Say hello to the Sunburst Arc, a galaxy in the small southern constellation Apus, whose light takes nearly 11 billion years to reach Earth—far, but not quite as far as the galaxies responsible for reionization. Two years ago, Emil Rivera-Thorsen of the University of Oslo and colleagues noticed that a particular wavelength of ultraviolet light from this galaxy appeared to sneak out through small gaps in its hydrogen gas, like water through a sieve. This light is not energetic enough to ionize hydrogen. But through those gaps, the team hypothesized, more energetic ionizing light might slip out as well.

Finding such a galaxy is rare, but the researchers' luck did not end there. The light of the Sunburst Arc has been bent and focused by the tremendous mass of a foreground galaxy cluster

acting as a natural lens, magnifying it a hundred times. To test their suspicions, the team directed the *Hubble Space Telescope* to the Sunburst Arc. In all 12 of the gravitationally distorted images, the researchers saw ultraviolet light capable of ionizing hydrogen blasting out of a small region within the galaxy. The team suspects that the ultraviolet radiation comes from a pocket of intense star formation no more than about 520 light-years across and is using one or a few holes in the surrounding gas to escape into intergalactic space.

Whether this actually is a missing piece in the reionization puzzle remains to be seen. “In the part of the Universe we studied, this is an atypical galaxy,” Rivera-Thorsen says. Out of hundreds of thousands the team has looked at, no other galaxy appears to behave this way. Whether such open pathways in the gas were more common in earlier galaxies is unknown. “That’s still an open question,” he says.

More studies with the *Hubble Space Telescope* are planned. “We are particularly looking forward to obtaining ultraviolet spectra in a range of wavelengths that includes the ionizing UV radiation emitted by so-called O-stars, which are the hottest (surface temperature above 30,000 kelvin), most massive (more than 8 times the mass of the Sun) and short-lived stars (life spans of 1/1000 times that of the Sun),” notes Dahle.

Compiled with material provided by University of Oslo. ★

The Pioneer Anomaly as a Coulomb Attraction

by Steven L. Morris, Professor emeritus, Physics Department
Los Angeles Harbor College, Wilmington, CA
(sandhnmorris@sbcglobal.net)

Abstract

The *Pioneer 10* and *Pioneer 11* spacecraft are decelerating at a greater rate than expected from purely gravitational forces. In this paper, it is argued that this Pioneer anomaly is due to the force of Coulomb attraction on the negatively charged spacecraft due to the positively charged cosmic rays passing through the Solar System.

Introduction

Radiometric tracking data of the *Pioneer 10* and *Pioneer 11* spacecraft at distances between 20 and 70 astronomical units from the Sun have shown a small, constant non-gravitational Doppler frequency drift of $df/dt = (5.99 \pm 0.01) \times 10^{-9}$ Hz/s, which can be interpreted as due to a constant acceleration of $a = (8.74 \pm 1.33) \times 10^{-10}$ m/s² toward the Sun (p. 1033 of Turyshev et al. 2005). Adopting their assumed mass of 241 kilograms (p. 1036) for each spacecraft when half of the hydrazine thruster fuel is gone, the force required to generate this anomalous acceleration is $F = (2.11 \pm 0.32) \times 10^{-7}$ newtons. Turyshev et al. (2005) investigate a wide range of possible causes of this anomaly, including the Lorentz magnetic force $F = qv \times B$, and conclude that this anomaly remains unexplained. Efforts to model the anomaly as due to thermal recoil are ongoing, as seen in Toth & Turyshev (2009) and in Turyshev et al. (2012).

It is worth investigating the contribution of the Lorentz electric force $F = qE$. The Sun may be expected to have an electric charge of +77 coulombs (Neslusan 2001), because the low mass of the electrons on the Sun's surface generates a larger population of electrons with the escape velocity compared to the slower thermal speeds of the protons. Morris (2006) calculated that the amount of electric charge the spacecraft would have to have would be unrealistically large but was worth checking as a pedagogical exercise.

However, there is a much larger pool of electric charge in the Solar System. May (2008) has pointed out that a pervasive electric field can exist in the heliosphere. Cosmic rays are high-energy particles from deep space that travel through the

Solar System at such high speeds they will be little deflected by gravitational acceleration. Approximately 90 percent of these particles are hydrogen nuclei, 9 percent are helium nuclei and only 1% are electrons, the lightweight electrons presumably having been deflected away from the Solar System by distant magnetic fields. At the great distances from the Sun experienced by the *Pioneer* spacecraft (beyond the planet Uranus), the sphere of positively charged cosmic rays centred on the Sun could exert a small but significant force of attraction on a negatively charged spacecraft.

Electric Charge in Interplanetary Space

The average fluxes of the two main components of primary cosmic rays at the top of the Earth's atmosphere are 640 hydrogen nuclei per square metre per second, and 94 helium nuclei per square metre per second (p. 86 of Friedlander 1989). Heavier nuclei are much less common and will be ignored in this analysis. These fluxes are for particles with energies above 1.5 GeV per nucleon (and speeds greater than 92% of the speed of light), arriving at the top of the Earth's atmosphere from directions within 30° of the zenith. These numbers imply a particle density of 3.45×10^{-5} hydrogen nuclei per cubic metre and 5.07×10^{-6} helium nuclei per cubic metre. Including the 1% population of electrons, the resulting charge density throughout interplanetary space is $+7.10 \times 10^{-24}$ coulombs per cubic metre.

Pioneer 10 was launched on 1972 March 2, and the data analyzed for the Pioneer anomaly were collected between 1987 January 3 and 1998 July 22, when the spacecraft was at a distance from the Sun of 40 AU to 70.5 AU respectively. *Pioneer 11* was launched on 1973 April 5, and the data analyzed for the Pioneer anomaly were collected between 1987 January 5 and 1990 October 1, when the spacecraft was at a distance of 22.4 AU to 31.7 AU respectively (Note 3, p. 1043 of Turyshev et al. 2005). Tables I and II list the amounts of cosmic-ray electric charge Q in the sphere interior to the location of the spacecraft, centred on the Sun. Assuming spherical symmetry of the cosmic-ray distribution, the electric charges exterior to the sphere will not exert a net force on the spacecraft. The Coulomb force law $F = k_e qQ/r^2$ can be rewritten to solve for the amount of charge q the spacecraft would have to possess to create the Pioneer anomaly. These are listed in Tables I and II as well.

Electric Charge on the Pioneer Spacecraft

The source of this negative charge for each spacecraft may be its radioactive fuel. The four RTGs (Radioisotope Thermoelectric Generators) had a pre-launch thermal fuel inventory of 2580 watts from Plutonium-238 undergoing alpha decay with a half-life of 87.74 years (Table IV of Turyshev et al. 2005),

with a decay energy of $5.5 \text{ MeV} = 8.8 \times 10^{-13} \text{ joules}$. A total of 2.9×10^{15} alpha particles would be emitted every second to provide such power, for a charge emission of $+9.4 \times 10^{-4}$ coulombs every second. The exponential decrease of this rate as the Plutonium-238 decayed can be easily calculated.

Of course, almost all of these alpha particles would be absorbed by the RTGs, but some would escape, and indeed the RTGs were placed on the opposite side of the spacecraft from the scientific instruments to reduce contamination. Even if only 0.0001% of the positively charged alpha particles escaped into space, a charge of -9.4×10^{-10} coulombs would be left behind every second. For *Pioneer 10*, a leakage of one in a million alpha particles from the RTGs would supply enough charge to create the Pioneer anomaly every 160 seconds and 100 seconds for the beginning and end dates respectively. For *Pioneer 11*, the times required would be 280 and 200 seconds respectively.

The consistency of these four times is encouraging, given that the Pioneer anomaly was measured from 22.4 AU to 70.5 AU. This calculation indicates that the Pioneer anomaly is due to Coulomb attraction, as long as a few minutes pass between the loss of electric charge from the Pioneer reactors and its recovery from interplanetary space. *

TABLE I	Start of Pioneer 10 Anomaly Measurements	End of Pioneer 10 Anomaly Measurements
Time from Launch (days)	5420	9638
Heliocentric Distance (AU)	40	70.5
Q (coulombs)	$+6.37 \times 10^{15}$	$+3.49 \times 10^{16}$
q (coulombs)	-1.32×10^{-7}	-7.47×10^{-8}
Charge Recovery Time (seconds)	160	100

TABLE II	Start of Pioneer 11 Anomaly Measurements	End of Pioneer 11 Anomaly Measurements
Time from Launch (days)	5023	6388
Heliocentric Distance (AU)	22.4	31.7
Q (coulombs)	$+1.12 \times 10^{15}$	$+3.17 \times 10^{15}$
q (coulombs)	-2.35×10^{-7}	-1.66×10^{-7}
Charge Recovery Time (seconds)	280	200

References

- Friedlander, M.W. (1989). *Cosmic Rays*. Cambridge MA: Harvard University Press.
- May, H.D. (2008). A pervasive electric field in the heliosphere. *IEEE Transactions on Plasma Science*, 36, 2876-2879.
- Morris, S.L. (2006). The Pioneer Spacecraft. *American Journal of Physics*, 74, 373.
- Neslusan, L. (2001). On the global electrostatic charge of stars. *A&A*, 372, 913-915.
- Toth, V.T. & Turyshev, S.G. (2009). Thermal recoil force, telemetry, and the Pioneer anomaly. *Phys. Rev. D* 79 (4), 043011, 1-10.
- Turyshev, S.G., Nieto, M.M., & Anderson J.D. (2005). Study of the Pioneer Anomaly: A problem set. *American Journal of Physics*, 73, 1033-1044.
- Turyshev, S.G., Toth, V.T., Kinsella, G., Lee, S., Lok, S.M. & Ellis, J. (2012). Support for the Thermal Origin of the Pioneer Anomaly. *Phys. Rev. Lett.* 108 (24), 241101, 1-5.

SERVING AMATEUR ASTRONOMERS FOR OVER 29 YEARS

toll-free 1-800-580-7160
 info@khanscope.com
www.khanscope.com

ALL MAJOR BRANDS, INCLUDING:
 AstroTrac • Meade • Celestron • Tele Vue • Kowa • Coronado • Levenhuk • ADM
 Sky-Watcher • Nikon • Kendrick • William Optics • Antares • Hotech • Farpoint
 Baader • iOptron • QSI • Telrad • TeleGizmos • Orion • Vixen • MoonLite • Lunt
 Explore Scientific • MallinCam • Rigel • Starlight Instruments • Vernonscope

SERVING BEGINNERS AND ADVANCED AMATEURS

**WE SHIP CANADA WIDE | WE ACCEPT TRADE-INS
 WIDE SELECTION OF NEW AND USED EQUIPMENT**

We service and repair most brands of telescopes and binoculars

TO ORDER TOLL-FREE, CALL **1-800-580-7160**
 OR LOCAL 416-783-4140
 OR ORDER ONLINE VIA OUR SECURE WEB SERVER AT **www.khanscope.com**

KHAN SCOPE CENTRE
 3243 Dufferin Street, Toronto, ON M6A 2T2
 in Toronto: 416 783 4140
 facebook.com/khanscope

**VISIT OUR SHOWROOM!
 OVER 70 SCOPES
 ON DISPLAY**

Playing with Magnitudes

by Gunter Hoernig, Okanagan Centre
hoernig@vip.net

One late evening in January, my wife and I wandered through the mountains and hills around Princeton in southern British Columbia. The sky was absolutely clear and studded with stars, the full Moon was out, and it was bitterly cold. But despite the chill it was a wonderful night. There was absolute stillness, only interrupted by the “crunch-crunch” of walking on the crusty surface of ice and snow. Some distance away the snowy hills and ridges gleamed in bright moonlight. It was a truly enchanting sight.

It was then that I envisioned this scene somewhat reminiscent of being on the surface of Pluto. Just imagining a thin atmosphere (and the “crunch-crunch” of walking on frozen CO₂), I thought the brightness on Pluto’s sunny side might just equal the brightness in this moonshine-drenched valley. Or would it?

Let’s see: Pluto is approximately 40 times further from our star than the Earth is, and taking the inverse square law of radiation, gives only 1/1600 of incident sunshine. In other words, distant Pluto only receives 0.0625% of the Sun’s energy as Earth does. That is not much, and certainly not enough to sit on a beach. But *how bright* would the Sun actually be on this remote world?

Although some astronomers refer to the old magnitude system as “burdensome and tricky,” it is not really that difficult to work with. And we do need it to solve the above problem. So, let’s give it a try.

We all know that on Earth the Sun’s brightness, expressed in magnitude, is -26.7 . (We should note, though, that “magnitude” is not an absolute quantity, but rather a ratio, just like the term “decibel” denotes ratios in electronics and audio. The magnitude system is a scale where increasingly positive values indicate lower brightnesses, with each successive magnitude being 2.512 fainter than the previous value.)

But how is the Sun’s magnitude of -26.7 actually determined? Simple: A zero-magnitude star such as Vega (actually magnitude 0.04) is used as a reference point. On Earth, Vega’s flux has been measured at $2.9 \times 10^{-8} \text{ W/m}^2$, and the Sun’s at 1390 W/m^2 . Hence the ratio of the two is 4.792^{10} . And since $\text{magnitude} = \log \text{ of ratio} \times 2.512$, filling in the numbers we thus have, $\log 4.792^{10} \times 2.512 = 26.7$, the Sun’s magnitude. Easy, isn’t it? But don’t take my word for it, check it out yourself!

So, what apparent magnitude would the Sun be on Pluto, then? As already mentioned, the solar flux on this remote world is 1600 times weaker than on Earth. Therefore, calculating the magnitude ratio of $1600 = \log 1600 \times 2.512$, equals 8.04. Subtracting this from the Sun’s brightness here on Earth, -26.7 minus -8.07 , we finally get our answer, which is magnitude -18.66 ! That is very, very bright indeed! In fact, it is 265 times as bright on the surface of Pluto as it would have been in the full moonshine of a Princeton valley.

Pluto, a dark and gloomy world? Forget it!

But how far must we travel to see the Sun at -12.6 , the visual magnitude of a full Moon on Earth? To find out, we can take the difference between -18.66 , the Sun’s brightness on Pluto, and -12.6 of the full Moon on Earth, which is 6.06. Calculating from this, the resulting brightness ratio is $= 2.512^{6.06} = 265$. To arrive at an actual distance then, all we have to do now is to take the root of 265, which is 16.27. And that is the answer—16 times further than Pluto, or some 640 astronomical units from the solar centre, way out in the Kuiper belt, the Sun will shine at magnitude -12.6 !

Even at this tremendous distance, the Sun, now only 3” across, would still be a dazzling object in the heavens, and much too bright to stare at safely. There would be plenty of light on a hypothetical body this far out, and future astronauts stomping through powdery methane crystals on the proverbial “Planet X” might marvel at the sights of gleaming ridges and jagged peaks—just as we did in an unnamed valley near Princeton on a cold January night. ★

RASC Internet Resources



Like us on facebook



Follow us on Twitter @rasc

www.rasc.ca

Visit the RASC Web site

www.rasc.ca/discussion

Email Discussion Groups

www.rasc.ca/contact

Contact the Society Office

www.rasc.ca/news

RASC eNews

Atmospheric Display of a Lifetime!

by Rick Stankiewicz, *Unattached*

2019 October 26 started out like any other fall day. It was a crisp -3°C and there was lots of fog south of Peterborough, Ontario, on the Otonabee River next to my home. I planned

to go fishing that day, but delayed my outing until after lunch, just to let the fog and mist dissipate.

Fortuitously, I spent the whole afternoon on the river and a thin layer of cirrus clouds started to drift in from the west later in the day. Around 4:15 p.m. I noticed the Sun lower in the west and I immediately recognized the “ring” (solar halo) around it and the sun dogs to either side. I have seen these many times over the years. From this point onward things went from ordinary to extraordinary.

The higher I looked the more unique things I saw. The clouds that drifted in this afternoon had just the right amount and configuration of ice crystals refracting and reflecting light to produce a sky show very few people at this latitude experience—a collection of ice halos and arcs rarely seen altogether (Figure 1). All this was clearly visible

Figure 1 (left)
— The show.

Figure 2 (right)—
Bottom to top
1) Parhelia (sun dogs),
2) Parhelic Circle,
3) 22 Degree Halo
(Solar Halo),
4) Upper Tangent Arc,
5) Upper Suncave
Parry Arc,
6) Supralateral Arc,
7) Circumzenithal Arc
(CZA).



to the naked eye, and the images I captured only hint at its true beauty. My friend Roger Mulligan used Smart Photo Fix to enhance the original image. He tried saturation, fill, and contrast to bring out more colour and details than I saw at the time of taking. The following is a list of what was visible over about a 30-minute period, while I watched various aspects brighten and dim as the clouds drifted by. All but two of these arcs were quite evident. I have included a labelled version of the same photo, which will assist in where to look to see these objects (Figure 2).

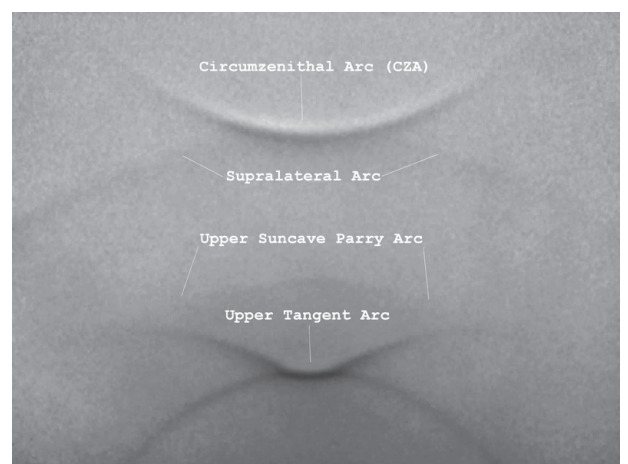
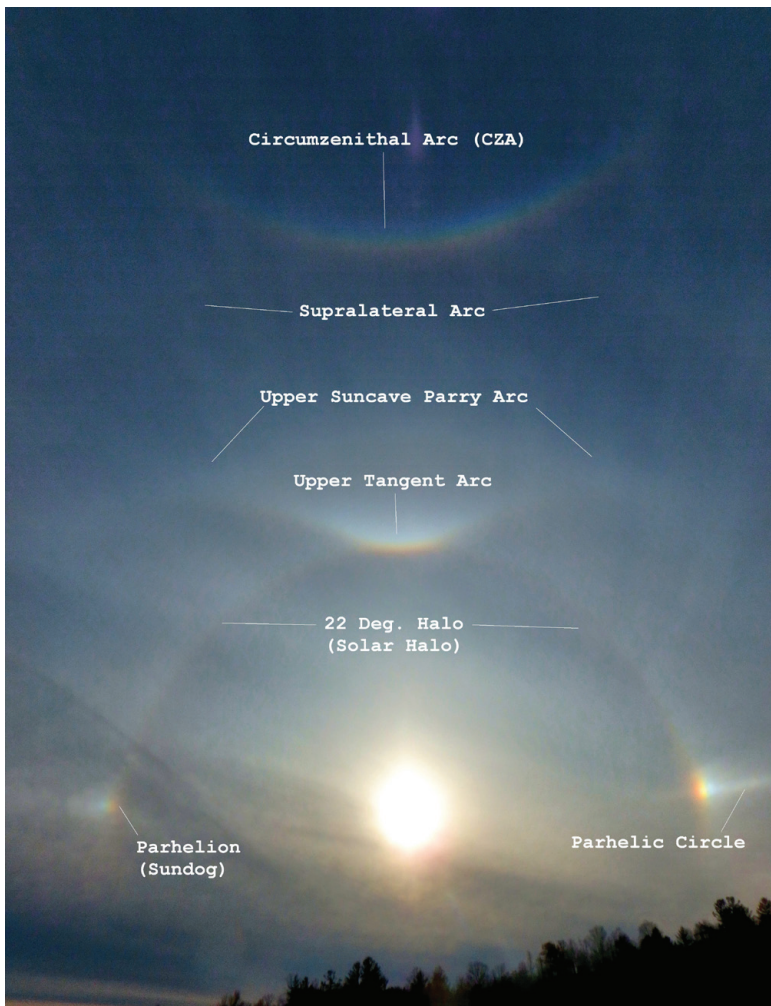
I suspected there might be more here than meets the eye, so I contacted a world-renowned atmospheric expert from the UK who I know (Les Cowley). I have dealt with Les over the years on various atmospheric questions. I sent him some of my images and asked for his opinion. He responded with not only a list that confirmed what was in my pictures, but even reprocessed my image that shows a close-up of the top four arcs. Two of these are only hinted at in my original images, but Les uses Affinity Photo and does a red-minus-blue colour subtraction that enhances all coloured halos. This gives a 3-D effect, bringing out faint details (Figure 3). To see more of Les

Cowley's work, check his websites: Atmospheric Optics: www.atoptics.co.uk and his Optics Picture of the Day (OPOD): www.atoptics.co.uk/opod.htm.

I have seen and photographed most of these phenomena over the years, most commonly solar halos (22° halo) and sundogs (perihelion), but the others less so. The Upper Suncave Parry Arc, named after Arctic explorer, Sir Wm. Edward Parry, who first recorded it during his 1819–1821 expedition, and supralateral arc, I had never seen before. So, to see them all together was a thrill to say the least. For me, this was an atmospheric display of a lifetime. It's only taken 63 years for me to see this one, so I am not holding my breath for another chance, but I won't stop looking.

Since I was fishing at the time of this event, I was ill prepared for recording it, so I had to do with what I had at the time, an Olympus "Tough" TG-860 (ISO 125; 1/2000 at $f/6$) and iPhone 5s for the close-up image.

We can marvel at what nature presents us, but to see it, we have to... "keep looking up." ★



Figures 3 (top) and 4 – Close up taken with an iPhone 5s camera.

Sidney Girling and Joseph Pearce at the Dominion Astrophysical Observatory

by Donald C. Morton

Herzberg Astronomy and Astrophysics Research Centre
National Research Council

Abstract

This concluding paper in recognition of the 100th anniversary of the Dominion Astrophysical Observatory describes the talented machinist Sidney Girling and the astronomer Joseph Pearce, who was Director from 1940 to 1951. In collaboration with the first Director, J.S. Plaskett, Pearce estimated the mass and dimensions of our Milky Way Galaxy, bringing broad international recognition to the observatory with their joint paper of 1934.

Introduction

Hanging on an office wall at the Dominion Astrophysical Observatory (DAO) in Victoria, B.C., is a staff photograph

reproduced in Figure 1. It must have been taken after September 1945 when Petrie and McKellar returned from their commissions as Lieutenant Commanders in the Royal Canadian Navy (Pearce 1946) and before early 1947, when Beals departed for Ottawa to be Dominion Astronomer. The location for the picture was the library at the northern end of the second floor in the original administration building prior to that area becoming offices in the year 2000 expansion. However, the large table still exists in the much-reduced library area on the southeast corner of the extended third floor.

Earlier articles have provided mini biographies of Carl Beals, Jean McDonald along with her later colleague Anne Underhill, Andrew McKellar, and then Bert Petrie and Ken Wright together (Morton 2018a, 2018b, 2019a, 2019b respectively), so this essay about Sidney Girling and Joseph Pearce completes the series. In the first and third of my previous contributions, I had identified the woman farthest right in the picture as the administrative assistant Jo-Anne or Joan Cooke, but recent discussions with Dennis Crabtree at the DAO and Richard Pearce, son of Joseph Pearce, have indicated that both the name and her responsibilities may be incorrect.



Figure 1 — The staff of the Dominion Astrophysical Observatory about 1946. Left to right around the table are the instrument maker Sidney S. Girling, the astronomers Robert M. Petrie, Joseph A. Pearce, Carlyle S. Beals, Andrew McKellar, Kenneth O. Wright, Jean K. McDonald and the unidentified staff member. (DAO photo)

Sidney S. Girling (1886–1982)

Sidney emigrated from England after the First World War and set up a small machine shop in Victoria, providing much useful service to the observatory that John Stanley Plaskett was establishing on Little Saanich Mountain. After 15 years providing contract services, Girling joined the DAO staff as Instrument Maker in 1943 (Pearce 1946, Hodgson 1989) and he retired in 1955. As recounted by Jack Heard (1970), Director of the David Dunlap Observatory, Plaskett himself had been a machinist in the Department of Physics at the University of Toronto before enrolling as a student there, so he recognized Girling's exceptional skills. Sidney contributed significantly to the operational success of the telescope and its instruments, culminating in the design and fabrication of the grating spectrograph initiated by Beals. Heard further notes that he invited Girling to Richmond Hill to spend two months in 1960 assisting Gerry Longworth in the design of the new grating instrument for the Toronto telescope.

During that time, Sidney occupied a second house on the mountain, across the road from where the Director Joseph Pearce lived with his wife and son. Richard Pearce (2019) has pleasant memories of times spent with Sidney, who made him a bow from a yew tree for archery practice and would take him fishing at nearby Beaver Lake using poles made from spirea bushes.

Before leaving England, Sidney and his brother Albert designed a three-wheeled delivery vehicle with a gasoline

engine and began production in 1912. The vehicle was successful, but not the business. After Sidney left for Victoria, Albert continued with automotive developments, including disc brakes carrying the Girling name that were particularly useful for racing cars.

Joseph A. Pearce (1893–1988)

Wright's (1989) detailed obituary records that Joseph Pearce (Figure 2) was born in Brantford, Ontario and studied mathematics and physics at the University of Toronto beginning in 1913. After war service as a signals officer, he returned to his studies in Toronto, receiving his B.A. in 1920 along with the Gold Medal of The Royal Astronomical Society of Canada and his M.A. in 1922. With a fellowship from the University of California in Berkeley, he began doctoral studies there in the fall of 1922, stopping enroute to visit the DAO (Pearce 1968). While at Berkeley, Pearce used the 36-inch refractor of the Lick Observatory to photograph the comet 1922c (Pearce 1923) and record spectra of the binary Delta Trianguli (Pearce 1924).

Two years later, in 1924, when Reynold K. Young left for a faculty position at the University of Toronto, Pearce joined the DAO staff. There he continued with his radial-velocity observations and analysis of spectroscopic binaries starting with orbits for both stars in the system HD 216014 (Pearce 1925). Binaries became a major component of his DAO research, resulting in the publication of the orbital details of at least 41 systems, many with both spectra measurable so that

the mass ratio could be determined. In three binaries, RZ Cas, 57 Cyg, and TX UMa, Pearce also derived the apsidal rotation of the semi-major axis caused by the gravitational distortion of one star by the other. Such data provide an important test of models of the internal structure of stars.

Figure 3 is an example of how Pearce (1959) determined important information about individual stars. This plot shows the radial velocities for the orbit of the eclipsing binary V477 Cygni with a period of 2.347 days and eccentricity of 0.235. Outside of eclipse the spectral lines of both components were measurable, permitting the determination of $M_1 \sin i$, $M_2 \sin i$ and $A \sin i$, where M_1 , M_2 , A and i are respectively the component masses, the semi major axis and the inclination of the orbital



Figure 2 — Joseph A. Pearce (1893–1988) and a micrometer microscope for measuring spectroscopic plates.

plane. An earlier analysis of the eclipses by Wallenquist (1949) provided the stellar radii as fractions of A and the inclination of 88.5 degrees so Pearce obtained a semi-major axis of 8.18×10^6 km and the following properties of the two stars:

	Primary	Secondary
Spectral Type	A3	F5
Radius	1.46 Suns	1.16 Suns
Mass	2.37 Suns	1.60 Suns
Mean Density	0.76 Suns	1.02 Suns

At the DAO, Pearce also began a very productive collaboration on the structure of our Milky Way Galaxy with the Director J.S. Plaskett, who wanted to extend to the B-type stars his observations of O-star spectra and the superposed narrow interstellar absorption lines of ionized calcium (Plaskett 1924). As explained by Broughton (2018), if the stars in the Milky Way disk are rotating about the centre with circular velocity decreasing with distance from the centre, their proper motions and radial velocities should display a double-sine curve with galactic longitude. Oort (1927) had developed a theoretical model and used stellar proper motions and radial velocities, including some from DAO, to estimate the parameters of galactic rotation. Thanks to a letter from Frank Schlesinger of Yale University, Plaskett realized how the DAO radial velocity measurements of more distant O and B stars could be especially helpful for determining the rotation of our galaxy, particularly the parameter that included the distance to the centre. Since the accuracy of radial velocities does not decrease with distance, unlike proper motions, the large distances of the faint O and B stars made them useful tools for detecting systematic differential galactic rotation relative to the random motions. An early result was enough observational material from the Victoria telescope for Pearce to complete his Ph.D. research and receive his degree from the University of California on the motions of the O and B stars (Pearce 1930).

In their first joint paper, Plaskett and Pearce (1930) reported on the analysis of 235 stars in which they had radial velocities for both the star and the interstellar absorption line of ionized calcium at 393.4 nm. (The weaker component of the calcium doublet at 396.8 nm often is not useful because it is blended with the broad H-epsilon stellar line of hydrogen at 397.0 nm.) They separated the stars into five distance groups, solved for the galactic rotation and found that, “for all except for the group of brightest and nearest stars, the rotational term for the stars is almost exactly twice that for the clouds, or the stars are at twice the mean distance of the clouds,” thus confirming the hypothesis that the interstellar gas is distributed uniformly. (Excited atoms and ions are very rare in the interstellar gas, so at visible

wavelengths we depend on the absorptions from the ground states of calcium and sodium because the corresponding lines of the abundant carbon, nitrogen, oxygen, and iron occur in the ultraviolet beyond the atmospheric cutoff.)

In their next paper, Plaskett and Pearce (1931) published the radial velocities for many of the stars they used in their investigations. It is noteworthy that 77% of those stars with three or more observations and not identified as a variable had probable errors of 2 km/sec or less in the velocity determination.

It was their third paper that established the international recognition of the DAO 16 years after the observatory began operations. Plaskett and Pearce (1934) analysed 849 stellar radial velocities, mostly from Victoria, and 881 proper motions, all from other sources, for stars of spectral types O to B7 and determined the following parameters for our Milky Way Galaxy:

Distance from Sun to centre	10 000 parsecs = 33 000 light-years	(24 000 light-years)
Diameter of galaxy	30 000 parsecs = 100 000 light-years	(300 000 light-years)
Rotational velocity at the Sun	275 km/sec	(230 km/sec)
Rotation period at the Sun	224×10^6 years	(200×10^6 years)
Total mass of our galaxy	1.65×10^{11} Suns	(10^{12} Suns)

For comparison the numbers from the 2019 *RASC Observer's Handbook* are listed in parentheses. Later observations of fainter stars have shown that our galaxy is three times larger than the 1931 estimate and six times more massive.

Pearce succeeded Edward Harper as Director of the DAO in 1940, continuing until 1951 when he resigned in favour of Robert Petrie in order to prioritize his own research on spectroscopic binaries until he retired in 1958.

Pearce was a regular contributor to this *Journal*, publishing 26 articles starting in 1921 when he was at the University of Toronto. From 1919 to 1922, he also was Chant's editorial assistant for the *Journal* (Pearce 1968). On settling in Victoria, Pearce was active with the RASC Victoria Centre and at the national level as well, becoming President during 1940–1941. He also was a Fellow of the Royal Society of Canada and President 1949–1950.

Beyond these scientific and administrative accomplishments, Carl Beals (1968), Pearce's colleague at the DAO for 19 years,

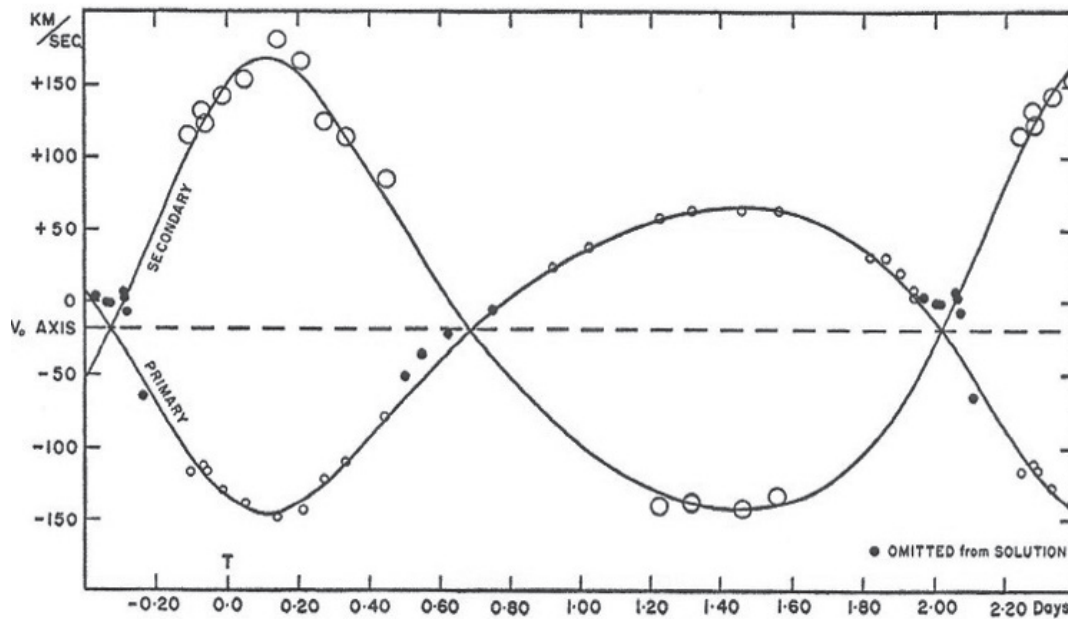


Figure 3 — The radial-velocity curves of the eclipsing binary V477 Cyg from Pearce (1959). The filled circles represent blended observations during the eclipses so were omitted from the analysis of the orbit. The large eccentricity of 0.235 distorts the usual sinusoidal curves of a circular orbit.

summarized his notable personal qualities, “Dr. Pearce was very popular with the young people at the observatory. In those days, as now, he had enormous energy and good humour and he would help anyone out of any kind of difficulty, scientific or otherwise—if he could—and he usually could because he was a very resourceful and active person.” ★

References

- Beals, C.S. (1968). Early days at the Dominion Astrophysical Observatory, *JRASC*, 62, 298–312.
- Broughton, R.P. (2018). *Northern Star J. S. Plaskett*, pp. 274–281, University of Toronto Press, Toronto, Buffalo, London.
- Heard, J.F. (1970). Sidney Girling, *David Dunlap Doings*, 3, No. 6.
- Hodgson, J.H. (1989). *The Heavens above and the earth beneath Part 1*, p. 149, Geological Survey of Canada.
- Morton, D.C. (2018a). Carl Beals and P-Cygni profiles, *JRASC*, 112, 112–115.
- Morton, D.C. (2018b). Early theoretical and digital research at the Dominion Astrophysical Observatory, *JRASC*, 112, 157–161.
- Morton, D.C. (2019a). Andrew McKellar and the temperature of space, *JRASC*, 113, 187–192.
- Morton, D.C. (2019b). Bert Petrie, Ken Wright, and the Dominion Astrophysical Observatory, *JRASC*, 113, 194–201.
- Oort, J.H. (1927). Observational evidence confirming Lindblad’s hypothesis of a rotation of the galactic system, *Bull. Astron. Inst. Netherlands*, 3, 275–282.
- Pearce, J.A. (1923). Observations of comet 1922c (Baade), *Lick Obs. Bull.* 11, 56–57.
- Pearce, J.A. (1924). The orbit of the spectroscopic binary Delta Trianguli, *Lick Obs. Bull.*, 11, 133.
- Pearce, J.A. (1925). The orbits of the spectroscopic components of H. D. 216014, *Publ. DAO*, 3, 171–178.
- Pearce, J.A. (1930). Motions of the O- and B-type stars, *PhD Thesis*, University of California.
- Pearce, J.A. (1946). Report of the Dominion Astrophysical Observatory for the years 1942–1945, *JRASC*, 40, 139–155.
- Pearce, J.A. (1959). The eclipsing variable H.D. 190786 (V477 Cygni), *Publ. DAO*, 10, 447–458.
- Pearce, J.A. (1968). Some recollections of the Observatory (1924–1935), *JRASC*, 62, 287–297.
- Pearce, R.M. (2019). private communication.
- Plaskett, J.S. (1924). The O-type stars, *Publ. DAO*, 2, 287–356.
- Plaskett, J.S. and Pearce, J.A. (1930). The motions and distribution of interstellar matter, *MNRAS*, 90, 243–268.
- Plaskett, J.S. and Pearce, J.A. (1931). The radial velocities of 523 O and B type stars obtained at Victoria 1923–1929, *Publ. DAO*, 5, 1–98.
- Plaskett, J.S. and Pearce, J.A. (1934). The distance and direction to the gravitational centre of the galaxy from the motions of the O5 to B7 stars, *MNRAS*, 94, 679–713.
- Wallenquist, Å. (1949). A photoelectric study of the eclipsing variable BD +31°3932, *Arkiv for Astronomi* 1, 59–67; *Med. Obs. Uppsala*, No. 96.
- Wright, K.O. (1989). Joseph A. Pearce, 1893–1988, *JRASC*, 83, 3–7.

Methods of Stellar Space-Density Analyses: A Retrospective Review

B. Cameron Reed

Department of Physics (Emeritus), Alma College

Abstract

Stellar space-density analyses, once a very active area of astronomical research, involved transforming counts of stars to given limiting magnitudes in selected areas of the sky into graphs of the number of stars per cubic parsec as a function of distance. Several methods of computing the transformation have been published, varying from manual spreadsheets to computer programs based on very sophisticated mathematical techniques for deconvolving integral equations. This paper revisits these techniques and compares the performance of seven of them published between 1913 and 2003 as applied to both simulated and real data.

Keywords: star counts, galactic structure, space-density analyses, (m , $\log \pi$) tables

Introduction

The origins of quantitative efforts to analyze the distribution of stars within the galaxy date to the late 18th and early 19th centuries with the work of William Herschel (1738–1822), who attempted to determine what he called the “construction of the heavens” by “star gauging.” By counting the numbers of stars to successively fainter magnitude limits in some 700 regions of the sky and assuming that all stars were of the same absolute magnitude, Herschel was able to deduce the relative dimensions of the galaxy, concluding that the Sun was near the centre of a flattened, roughly elliptical system extending about five times further in the plane of the Milky Way than in the perpendicular direction. This work was carried on by his son, Sir John Herschel (1792–1871), who used stellar parallaxes to establish the first evidence of an intrinsic distribution of stellar absolute magnitudes—the Luminosity Function (LF). German astronomer Hugo von Seeliger (1849–1924) put stellar distribution analyses on a firm mathematical footing by establishing integral equations relating the run of density of stars as a function of parallax (distance) to the number appearing in a given interval of apparent magnitude, as well as procedures for correcting the apparent distribution of stars for the effects of interstellar extinction.

What might be termed the “classical golden age” of stellar distribution analyses reached its zenith in the first quarter of the

20th century with the work of Jacobus Kapteyn (1851–1922) at the University of Groningen. Kapteyn initiated a plan to obtain star counts, magnitude estimates, spectral classifications, proper motions, and radial velocities for about 20,000 stars in some 200 “Selected Areas” distributed around the celestial sphere. The resulting picture of galactic structure, the “Kapteyn Universe,” was published in *The Astrophysical Journal (ApJ)* shortly before his death (Kapteyn, 1922), and depicted a Sun-centred lens-shaped structure about 16 kiloparsecs in diameter with an axial-to-polar ratio of about 5:1. Kapteyn noted that the system could not be in a steady state unless there was a general rotational motion around the galactic polar axis, and also that, when the work was further developed, it might be possible to “...determine the amount of dark matter from its gravitational effect.” While he surely had in mind ordinary but non-luminous matter as opposed to current particle-physics concepts of dark matter, his remark was prescient.

The subsequent discoveries of interstellar extinction, galactic rotation, and different stellar populations radically altered astronomers’ ideas of galactic structure, but Herschellian star gauging continued to be of value. Space-density analyses entered a second golden age in the post-WWII period, in particular through the efforts of American astronomer Sidney W. McCuskey (1907–1979) and his collaborators and students at the Case Institute of Technology in Cleveland, Ohio (later and still Case Western Reserve University). McCuskey undertook, from 1945 onward, an extensive series of stellar-distribution analyses with the goal of determining the galactic structure within 1500 parsecs of the Sun. In his last publication, which appeared posthumously, McCuskey analyzed data for over 8000 stars in a field of sky in the Centaurus–Crux region of the southern sky (McCuskey, 1983).

The raw data for these studies were apparent magnitudes and spectral classifications for hundreds or thousands of stars in some target area of the sky that usually covered a few or tens of square degrees. These were usually acquired by calibrating and examining photographic plates obtained with wide-field Schmidt telescopes. The stars would be segregated into relatively narrowly defined groupings of spectral types (for example, B8–A0 dwarfs; the reason for this is described in more detail below), and counts made of the number of stars that appeared in given ranges of apparent blue (B) or visual (V) magnitude. For practical purposes, the objective-prism spectra obtained in such studies could be reliably classified to $V \sim 13$.

Turning these data into runs of the stellar space density required two steps. First, and the main focus of this paper,

it was necessary to “deconvolve” the star counts to produce a so-called “fictitious” density function, the run of density versus distance neglecting any interstellar extinction. The second step was to correct the fictitious densities for the effects of extinction by using information on stellar colours to determine the run of extinction versus distance; this was usually done by studying intrinsically bright O- and B-type stars in the field of interest, which could be detected to great distances.

As might be imagined, both steps were fraught with statistical uncertainties. At bright and faint magnitudes, the counts could be small in number due to a sheer lack of nearby stars and running up against the effects of detectability limits. Whatever uncertainties were baked into the fictitious densities would then be compounded in modelling the run of extinction. There was by no means any guarantee that extinction would be a smooth function of distance: Nature might be so insensitive to the needs of astronomers as to distribute interstellar clouds and dust in globules and sheets between the Sun and the stars under study.

My purpose in this paper is to examine the relative merits of various methods that were developed to determine the run of fictitious density; I do not concern myself with the issue of extinction corrections for the reasons adduced above.

The fundamental difficulty in determining the fictitious densities is that since the star counts are related to the density by an integral equation [see Equation (2) below] with the desired density function residing *within the integrand*, the density function $\rho(r)$ is not uniquely related to the number of stars as a function of apparent magnitude. This situation renders multiple solutions possible, with no infallible way of telling which is the “true” one. Various approaches to recovering the density distribution were developed, often reflective of the computational technology of their time.

The outline of this paper is as follows. In Section 2, I give a brief summary of the fundamental integral equation of stellar statistics that incorporates the desired density function and hand-computation methods of solving it. Section 3 summarizes seven solution methods that have been developed over nearly a century. To compare these as uniformly as possible, I have developed programs for generating simulated star counts corresponding to assumed density and luminosity functions; this is described in Section 4. Results of the comparisons are presented in Section 5, and Section 6 applies what appears to be the best methods to two examples of real data. Some brief closing remarks appear in Section 7.

The Integral Equation of Stellar Statistics, ($m, \log \pi$) Tables, and The Revival of Star Counts

As described above, let $\rho(r)$ represent the number of stars per cubic parsec of the restricted range of spectral types under consideration as a function of fictitious distance r in some direction of interest. A thin spherical shell of space of thickness dr at distance r will then contain a total of $4\pi r^2 \rho(r) dr$ stars. For practical purposes one will be able to image only so many square degrees of sky, usually designated as Ω . The total number of square degrees on the celestial sphere is 41253, so this reduces the count in a distance shell to $(4\pi\Omega/41253)r^2 \rho(r) dr$ stars. At this point the *Luminosity Function* (LF) is introduced, usually designated as $\Phi(M) dM$, which gives the fraction of stars of the type under consideration that have absolute magnitudes M between M and $M + dM$. With this, the number of stars in the shell that will appear to have *apparent* magnitudes between m and $m + dm$ will be $(4\pi\Omega/41253)[F(M)dM]r^2 \rho(r) dr$, where M , r , and m are linked by the usual distance-modulus equation,

$$m - M = 5(\log r) - 5. \quad (1)$$

Formally, $\Phi(M)$ should be written as $\Phi(M, r)$.

Integrating over all space with M , r , and m related in this way at every distance gives the total number of stars that will appear to have *apparent* magnitudes between m and $m + dm$, usually designated as $A(m)$:

$$A(m) = \frac{4\pi\Omega}{41253} \int_0^{\infty} F(M) r^2 \rho(r) dr, \quad (2)$$

where dM has been written as Δm in recognition of the fact that for practical purposes the ranges of apparent magnitudes will be finite; typically, $\Delta m \sim 0.5$ mag. Equation (2) is known as the Fundamental Integral Equation of Stellar Statistics.

The reason that a restricted range of spectral-luminosity types is considered is to narrow the range of absolute magnitudes that will dominantly contribute to $\Phi(M)$, and thus hopefully return sharper resolution in determining $\rho(r)$. In most restricted-type studies the LF was usually assumed to be Gaussian with a mean absolute magnitude M_0 and dispersion σ :

$$F(M) = \frac{1}{s\sqrt{2\pi}} \exp\left[-\frac{1}{2s^2}(M - M_0)^2\right]. \quad (3)$$

Equation (2) is an example of what is known to mathematicians as a convolution problem: the function to be determined, $\rho(r)$, lies within the integrand and is *convolved* with $\Phi(M)$. While mathematicians have been studying integral equations for well over a century and have devised numerous ways of addressing them, the fundamental stumbling block is that the problem is ill posed: Different possible solutions for $\rho(r)$ can sensibly reproduce the stars counts (say, within their Poisson errors), so there is no unique solution for $\rho(r)$. Since star-count data can be plagued by small-number statistics that carry inherently large relative errors, the situation becomes even more tangled.

As an example of the problems that can arise in determining $\rho(r)$, consider the following very straightforward approach to solving equation (2). Suppose that the star counts are specified for K values of m , that is, one has $A(m_j)$ with $j = 1$ to K . Treat the counts as a one-column matrix $[A(m_j)]$ of K rows. Divide space up into some sensible number of shells of distance r_i , with $i = 1$ to N , and consider the values of the stellar density at each distance, $\rho(r_i)$ as a one-column matrix of N rows, $[\rho(r_i) r_i^2]$, whose elements incorporate the $4\pi m/41253$ prefactor in equation (2). Then construct a matrix of dimension N rows by K columns, $[\Phi_{ij}]$, whose elements are computed from the luminosity function with $M = m_j - 5(\log r_i) + 5$. Invert $[\Phi]$, multiply it into $[A(m_j)]$, and *voilà*: out pops $[\rho(r_i)]$. The problem that inevitably arises with this approach, however, is that the results often include physically absurd negative densities. Least-squares-type minimizations of the differences between predicted and observed star counts also tend to generate negative densities. The underlying problem is that the mathematics is ignorant of the physics and does not know that negative densities are impossible.

Analytic solutions to extracting $\rho(r)$ were developed early on (see below), but their inflexibility drove early researchers to a labour-intensive manual-spreadsheet method known as an $(m, \log \pi)$ table. This approach effectively mimicked the matrix approach, but with a human being at the helm whose job was to ensure realistic densities. In the spreadsheet, rows correspond to apparent magnitude and columns to shells of volume set out in increments of equal spacings of $(\log r)$, which ran over a range of distances sensible to the data at hand. The “ $\log \pi$ ” nomenclature arose from the fact that stellar distances could be determined via trigonometric parallaxes, whose values were always designated by π . The user would first calculate a matrix of values of Φ according as the apparent magnitudes and distances corresponding to the elements of the spread-

sheet. Then an initial guess as to the density distribution would be made, say by assuming a uniform density over all distances. Predicted star counts would be generated and compared to those observed, and a lengthy iterative process of adjusting the density distribution would then follow until the predicted and observed counts were in reasonable agreement. Details of this procedure are laid out in classic texts by Bok (1937), Trumpler and Weaver (1953), Mihalas and Routly (1968), and Mihalas and Binney (1981), but, as might be imagined, there was no small amount of subjectivity involved.

From the 1960s through the 1980s, approaches to star-count analyses underwent two major revisions. First, the arrival of mainframe and later personal computers meant that humans could be freed from the drudgery of manual calculations, and several algorithms for solving equation (2) were advanced. As described in the following section, some of these reached levels of mathematical sophistication that were probably unjustified in view of the nature of the input data. This author admits to developing one such technique (Reed 1983), an indiscretion I now attribute to the youthful misconception that a closed-form mathematical solution to a physical problem must always be preferred. The second revision saw the emergence of an entirely new philosophy of the role of star counts. This was that instead of using measured counts with all their statistical noisiness to try to work backwards to $\rho(r)$, approach the problem from the other direction by *assuming* a model of the galaxy that comprised various components (thin disk, thick disk, halo, ...), *predict* star counts, and then adjust the model as necessary. This change was prompted by evolutions in technology, which brought forward high-speed plate-scanning machines, efficient large-area CCD detectors, the troves of data that could be acquired with ever-larger ground- and space-based telescopes that could reach very faint limiting magnitudes and which have culminated in the *HIPPARCOS* and *Gaia* missions measuring parallaxes directly. As examples of such models, see Bahcall & Soneira (1980) and Pritchet (1983) and references therein. Bahcall (1986) remarked that star counts “...were a subject whose time had passed and come again.” With these developments, the classical $(m, \log \pi)$ -type approach rapidly faded into history.

While describing some of this history to a group of students, I began to wonder if the various density-recovery methods that had been developed had ever been directly tested head-to-head by feeding them simulated data derived from an assumed-known density distribution. A search of the literature turned up seven methods that could readily be programmed and

compared, including two published by myself. While some papers reported comparisons between methods, none ever undertook a comparison of all of them with the same data. As described in the following section, two other methods have also been published, but I disregard them for various reasons.

Before proceeding to describe these methods, another remark on the nature of density-recovery techniques is appropriate. Suppose that we are working with a Gaussian LF as in equation (3); this is in fact assumed to be the case in generating the simulated data in Section 4 below. There is a 50% chance that a given star will have an absolute magnitude brighter (fainter) than the mean absolute magnitude M_o . For a given apparent magnitude, this means a 50% chance that the star will be inferred to be more (less) distant than the nominal distance r_o corresponding to M_o . However, the impact of this on the density distribution is asymmetric. If the star is imagined to be closer than r_o it will lie in a smaller volume of space than if it is more distant, which causes the inferred stellar density at nearby distances to be greater than is actually the case. Conversely, the range of distances available for fainter magnitudes (distances greater than r_o) is unlimited, with the result that inferred density distributions will inevitably exhibit long low-density exponential tails. These effects cause the distance distribution for an individual star to have a mean distance value $\langle r \rangle$ greater than r_o , namely $\langle r \rangle = r_o e^{\prime}$, where $\prime = (s \ln 10)^2 / 50$, while having a most probable distance of $r_{mp} = r_o e^{-2\prime}$ and making a maximum contribution to the run of density at $r_{max} = r_o e^{-6\prime}$. For values of σ normally adopted in density analyses, these values do not differ wildly from r_o (for example, $r_{max} \sim 0.85 r_o$ for $\sigma = 0.5$), but do cause the distance distribution inferred for all stars to be asymmetric. These “front-loading” and “exponential tail” asymmetries are built into every stellar density analysis but were often not explicitly acknowledged in practice. These effects may have contributed to McCuskey’s (1965) observation in a review article on galactic structure that “...there is evidence from the general star counts for a somewhat elongated relatively high density region near the sun with its maximum about 300–500 parsecs from the sun and toward the galactic anti-center.”

Stellar Density Analysis Methods

The seven methods alluded to above are summarized here, in chronological order of publication.

3.1 Eddington (1913)

Eddington (1913) developed a direct solution to equation (2) by a Taylor-series expansion method. His notation is

somewhat confusing; good summaries of his approach appear in Spaenhauer (1977) and Ochsenbein (1980).

This method assumes a Gaussian LF of dispersion σ . If $A(x)$ is the number of stars with distance modulus $m - M$ between x and $x + dx$, then the true number of stars $T(x)$ with distance moduli between these limits is given by

$$T(x) = A(x) - \frac{s^2}{2} \left(\frac{d^2 A}{dx^2} \right)_x + \dots \quad (4)$$

The second derivatives of the star counts can readily be computed via the differences of successive counts,

$$\left(\frac{d^2 A}{dm^2} \right)_m = \frac{1}{Dm^2} [A(m + Dm) + A(m - Dm) - 2A(m)]. \quad (5)$$

This method is very amenable to spreadsheet computation. Star counts as a function of magnitude are laid out in the rows of the spreadsheet. The x value of each row is determined from $x = m - MO$, and distances corresponding to the inner and outer limits of each magnitude bin are computed from $x + \Delta m/2$. Each magnitude bin thus corresponds to a spherical shell whose volume can be computed on accounting for the areal coverage Ω involved, and values of $T(x)$ can be directly converted into densities for each bin. In addition to assuming a Gaussian LF, the limitations of this method are that the second derivatives may be erratic, and that densities can be computed only at distances corresponding to the centres of the count bins.

3.2 Crowder (1959)

This method seems to have been the first explicitly developed for its adaptability to machine computation. If it is assumed that the density distribution follows the description

$$r(r) = \exp \left[a + b(\ln r) + c(\ln r)^2 \right], \quad (6)$$

then equation (2) can be integrated directly in the case of a Gaussian LF with the result that the star counts will behave as

$$\ln A(m) = C_1 + C_2 m + C_3 m^2. \quad (7)$$

The coefficients (a, b, c) can be determined in terms of (C_1, C_2, C_3) ; a parabolic fit to $\ln A(m)$ then automatically determines the run of density. This approach was used extensively in the

Case/McCuskey studies mentioned above. While it has the advantage of computational convenience, there is obviously no *a priori* guarantee that the density profile will behave as equation (6); indeed, such a prescription can at most accommodate only a single maximum in $\rho(r)$, at $\ln r = -b/2c$. With the curve-fitting routines built into modern spreadsheets, this method is also easily programmed on a desktop computer.

3.3 Dolan (1974)

This method was also developed at Case Western Reserve University and involves an approach that derived from computations involved in analyses of astronomical X-ray spectra. The LF is again assumed to be Gaussian. Dolan's notation and description can be confusing in places, but he does give a detailed example against which users can check their own implementations. This method, which is also very easy to set up on a spreadsheet, includes a "smearing" matrix that corresponds to the spread of the LF and that in effect leads to a sort of running average of counts over distance bins in a manner similar to Eddington's second-derivative technique. In practice, I have found that the two methods produce very similar results.

3.4 Gschwind (1975)

This method is very computationally intensive but requires no specific form for the LF. For each star in the sample a random absolute magnitude is generated, consistent with the LF. With each stellar distance then (presumed) known, the density distribution is computed. This "Monte Carlo" process is then repeated numerous times (Gschwind suggested 100 trials), allowing one to determine a mean density distribution and estimate the associated uncertainty.

3.5 Reed (1983)

This technique also assumes a Gaussian LF and involves a direct analytic solution to equation (2). First, the common logarithms of the star counts are fit by a linear function,

$$\log A(m) = s_0 + s_1 m . \quad (8)$$

The fit need not be particularly good; the only purpose of this step is to determine the coefficients s_0 and s_1 . The star counts are then reduced to be all on the order of unity by the transformation

$$A^*(m) = A(m) 10^{-(s_0 + s_1 m)} . \quad (9)$$

These reduced counts are then fit with a polynomial of order up to a few. With the star counts in this form, equation (2)

can be transformed into a form where the density function emerges as a sum of Hermite polynomials whose expansion coefficients are related to the coefficients of the polynomial fit to the $A^*(m)$.

When I first developed this method, I tested it against some simulated data, achieving positive results. While my memory is now vague as to exactly how I generated the simulated data, I do not now believe that this was a rigorous test. The data were likely simulated counts generated by a numerical integration scheme as opposed to generating a list of individual simulated apparent magnitudes and then binning; the method likely essentially reproduced what was input to it. More rigorous—and unfortunately less encouraging—tests are described in the following section.

3.6 Reed (1985)

This method is a computerized version of the traditional hand-computed $(m, \log \pi)$ table that is not only much faster than a manual computation but removes most of the subjectivity that can be introduced by a human operator. The key to this method is a very general, intuitively appealing iterative approach to solving integral equations published by Lucy (1974), which has been cited over 1500 times. A great advantage of this approach is that if the user's initial guess for the density distribution is positively valued, all subsequent estimates will be as well. At each step, predicted star counts are compared to observed ones, and the density distribution is refined to bring the two into closer alignment. The user selects both the maximum number of iterations allowed, and, as in a traditional $(m, \log \pi)$ table, the stepsize in $(\log r)$. From experimenting with this method over many years I have found that only a few iterations (generally ~ 10) are required to bring as many of the predicted counts within the Poisson errors of the actual counts as can be sensibly had without introducing wild oscillatory variations in the density distribution that are unlikely to be physically realistic. For $\Delta(\log r)$, a value on the order of 0.05 usually gives a sensible number of volume shells. No specific LF is assumed.

3.7 Branham (2003)

This matrix-based approach utilizes the mathematics of Regularized Total Least Squares, which is particularly effective for addressing systems of ill-conditioned linear equations. No specific LF is assumed. Like the Reed (1985) method above, this method is iterative, with the user adjusting a quantity known as the "ridge parameter" (designated as τ),

generally adjusting it upward until no negative values of the density appear and the density distribution looks reasonable. (If negative densities do appear, they should be tolerated only at the brightest and faintest magnitude bins, where the relative errors in the counts are large). For reasons explained by Branham, the ridge parameter can take quite large values. The matrix mathematics underlying this method are involved, but Branham presents a very explicit recipe for implementing the method. In view of the fact that the sizes of the matrices involved will vary from case to case, this method is best implemented with a program where these can readily be varied, as opposed to using a spreadsheet.

Two other published methods are not used here: Spaenhauer (1978) and Ochsenbein (1980). Spaenhauer developed a least-squares matrix approach, but concluded on the basis of test data that "...when we do not know *a priori* the location of a density maximum [spiral arm], it is very doubtful whether the star numbers obtained...are reliable." In the case of Ochsenbein, I must confess to finding his mathematics to be impenetrable; his method does not seem to have been used in practice.

In comparing these methods in what follows, I do not concern myself with comparing their approaches to computing uncertainties in the density estimates (which can be very mathematically elaborate), or with more subtle effects such as the Malmquist bias.

Simulated Data

To test the above routines, I have generated simulated data corresponding to two assumed density distributions. To generate this data, I wrote a master program in which the desired density distribution $\rho(r)$ is programmed into a subroutine. The LF is assumed to be Gaussian, with values of M_o and σ specified by the user; this could be altered if desired. The user also specifies the simulated survey area Ω and the distance limit r_{max} to which calculations are to be carried out.

The program begins by first numerically integrating $\rho(r)$ out to the specified distance limit to determine the number of stars N to simulate; this is done with a 2000-slice Simpson's rule subroutine. This subroutine also determines the maximum value of $r2r(r)$; call this $[r2r(r)]_{max}$. Generating a distribution of distances that respects the density distribution is done within another loop, which, upon each execution, calls the computer's built-in random-number generator to create a pair of random numbers, (x, y) , both in the range $(0, 1)$; x is scaled to be in the range $(0, r_{max})$ to create a trial distance r_{trial} .

The value of $r^2_{trial}\rho(r_{trial})$ is computed, and if the "paired" y lies between 0 and $r^2_{trial}\rho(r_{trial})/[r2r(r)]_{max}$, then the distance is taken as valid. If the random distance is deemed invalid, the loop executes again until a valid one is found. This process is repeated as many times as necessary until distances for all N stars have been generated. This generates a list of distances consistent with the assumed density distribution since the number of stars at any distance will be proportional to $r2r(r)$. A similar loop then generates as many absolute magnitudes according to the specified LF by sampling absolute magnitudes within ± 3 standard deviations of M_o . Each absolute magnitude is assigned to a star, and corresponding apparent magnitudes are computed. A file of all data is produced, and a separate program bins the star counts according to bin centres and widths specified by the user. Since a finite number of stars are generated, there will naturally be some noise in sampling the assumed density distribution; only if an effectively infinite number of stars were used would the distribution be smoothly sampled.

The first assumed distribution is a simple one, but likely to prove a challenge for any deconvolution method: no stars out to a distance of 100 pc, then a uniform density of one star per 100 pc³ out to 500 pc, and none at greater distances. I assumed $M_o = 0$, $\sigma = 0.5$, and $\Omega = 20$ square degrees, which give $N = 2520$, a largish but not unreasonable sample for a traditional analysis.

The second assumed distribution has an exponentially decreasing "background" density punctuated by a Gaussian-shaped "spiral arm" at a specified distance. The functional form is

$$r(r) = Ae^{-(r-r_0)/B} + Ce^{-(r-r_1)^2/D} \quad (10)$$

where A, B, C, D, r_0 and r_1 are set by the user. In the test described below I adopted $(A, B, C, D, r_0, r_1) = (0.05 \text{ stars/pc}^3, 300 \text{ pc}, 0.03 \text{ stars/pc}^3, 10^4 \text{ pc}^2, 0 \text{ pc}, 500 \text{ pc})$ with a limiting distance of 1000 pc. With $M_o = 5$ (similar to that of the Sun), $\sigma = 0.5$, and $\Omega = 5$ square degrees, N emerges as 4726 stars between magnitudes 6.4 and 16.3. This is a large number for a traditional analysis but should give the routines enough data to converge on stable solutions.

Comparing the Methods—Simulated Data

Spreadsheets or FORTRAN programs were written for each of the above methods: the former for the Eddington, Crowder, Dolan, and Reed (1983) approaches, and the latter for the others. The author would be happy to distribute copies of the spreadsheets and codes to any interested reader.

For the uniform-density model, the star counts were binned into thirteen half-magnitude intervals centered on $m = 4.0$ (0.5) 10.0. For the Reed (1983) Hermite-polynomial method, a sixth-order fit was performed to the reduced star counts. For the Gschwind method, 1000 Monte Carlo trials were performed, and for Branham's method a ridge parameter value of 10^6 was used; this resulted in only some very slight negative densities beyond distances of 600 pc. For the Reed (1985) automated routine, $\Delta(\log r) = 0.05$ was adopted.

As can be seen in Figure 1, the Crowder, Gschwind, and Hermite-polynomial methods all produce terrible results, exhibiting serious front-loading and long exponential tails.

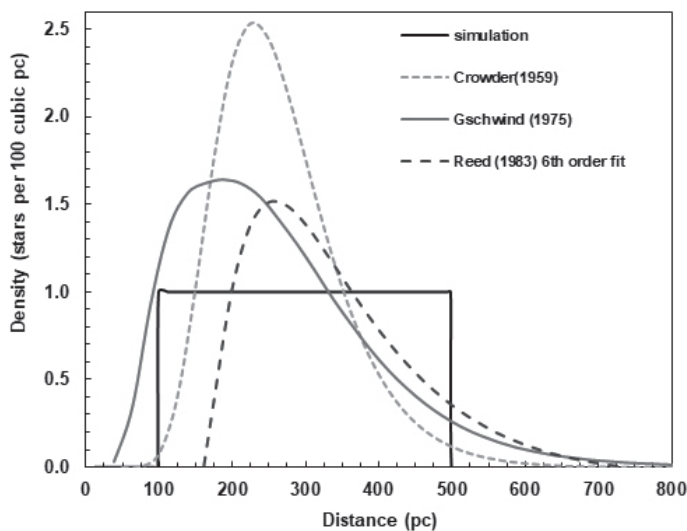


Figure 1 — Results of star-count analyses for uniform-density model. See also Figure 2.

The Eddington, Dolan, Reed (1985), and Branham (2003) methods performed more respectably (Figure 2), with the Eddington and Dolan methods generating practically identical results.

In the case of the dual-exponential model, the situation is the same: Crowder, Gschwind, and Reed (1983) turn in abysmal performances, while Eddington, Dolan, Reed (1985) and Branham do respectable jobs of capturing the Gaussian maximum in the density at 500 pc, if one disregards oscillations at nearby distances (Figure 3). Branham captures the location and value of the maximum most closely but puts secondary peaks at about 275 and 800 pc; these are not likely to be of great statistical significance. The value of the ridge parameter here is $\tau = 70,000$, essentially the lowest value that gave no negative densities. Reed, Dolan and Eddington all

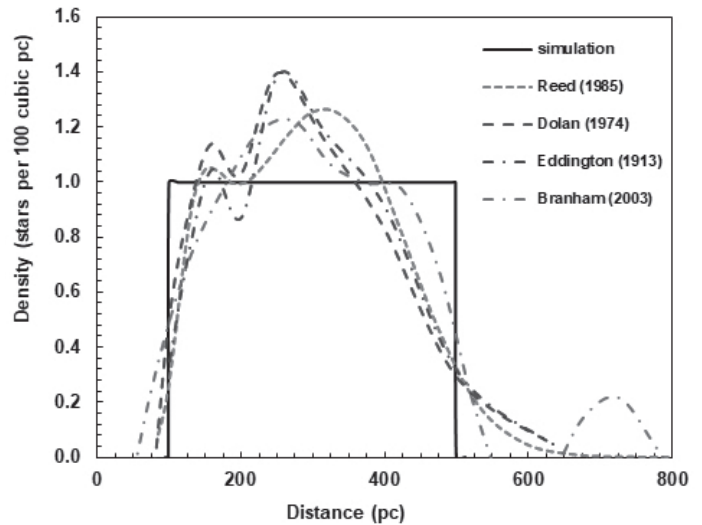


Figure 2 — Results of star-count analyses for uniform-density model.

place the peak density at about 450 pc (not far from the r_{\max} position described above), with Reed's density run being the smoothest of the three: 15 iterations gave 16 of 21 star-count values reproduced within their Poisson errors. All three of these latter methods underestimate the maximum density by about 20%, a manifestation of the front-loading/exponential-tail phenomena.

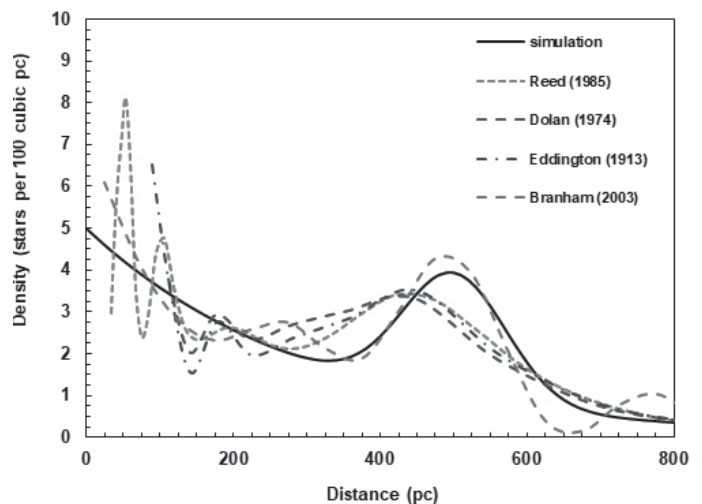


Figure 3 — Results of star-count analyses for the double-exponential model of Equation (10).

Based on these tests, Branham's method seems to have the edge, with the old-school Eddington and automated ($m, \log \pi$) methods not far behind. In both Eddington's and Dolan's methods it is not clear from their papers how non-Gaussian luminosity functions would be accommodated.

Comparing the Methods – Real Data

6.1 South Galactic Pole M-Dwarf Data

In a paper published shortly after Dolan's (1974) paper, Thé and Staller (1974) examined the distribution of M-type dwarfs in the direction of the south galactic pole. Their overall sample comprised 96 M2–M4 dwarfs in a 238-square-degree region with photographic magnitudes between about 12.5 and 16. Upon eliminating a few extremely faint stars of uncertain spectral type and a few high-velocity stars, they were left with 82 objects on which they performed a traditional ($m, \log \pi$) analysis (apparently by hand), assuming an average absolute magnitude $M_{pg} = 12.25$ and dispersion $\sigma = 0.5$ mag. Since all of these stars are nearby, no corrections for interstellar extinction were applied. Their analysis revealed a maximum density of about four stars per 100 pc³ at $r \sim 20$ pc, and an average density of about three stars per 100 pc³ beyond this distance. On accounting for various selection effects, they estimated that the true average density would be closer to about six stars per 100 pc³. This paper garnered attention at the time because their average density was significantly lower than that found by Murray and Sanduleak (1972) for the same type of stars in the direction of the north galactic pole, about 12 stars per 100 pc³.

Dolan (1975) re-analyzed the Thé and Staller data (83 stars) with his technique, finding a considerably higher peak density of about nine stars per 100 pc³ at $r \sim 15$ pc, and concluded that the density was not necessarily in conflict with Murray and Sanduleak's result. In my 1985 automated ($m, \log \pi$) paper, I also analyzed this data (81 stars), similarly finding a peak density of about nine stars per 100 pc³, but at $r \sim 20$ pc as opposed to Dolan's 15 pc. Unfortunately, Dolan did not tabulate his star counts, so we have no way of knowing exactly what were his input data; I have been unable to contact him. Branham also analyzed this data, using 83 stars (see his Table 3), finding a lower peak density of about four stars per 100 pc³ at $r \sim 20$ pc, although followed with a less rapid decline at greater distances than Thé and Staller had found.

I have re-analyzed the Thé and Staller counts as tabulated by Branham using my implementations of the Eddington, Dolan, and Branham methods as well as my 1985 method. The results are shown in Figure 4, along with Thé and Staller's original results. It is not clear to me why my implementation of Dolan's method gives different results from his 1975 paper; my spreadsheet for his method reproduces exactly the results of his Table 1 in his 1974 paper, an analysis of B8–A3 stars in the galactic plane. My implementation of Branham's method also predicts a higher peak density than did he, by about a

factor of two. This may be due to different choices of his ridge parameter; my results are for $\tau = 114,000$, which gave only one very slight negative density, at $r = 5$ pc. I have contacted Dr. Branham, who was unfortunately unable to recover his notes from the time he was working on this problem and could not recall exactly what ridge parameter or form he used for the Luminosity Function. His estimates of the uncertainties in the derived densities run to about $\pm 50\%$ however, so the discrepancy is likely not as drastic as it appears. I find that if I use a slightly brighter average absolute magnitude (12.0 vs. 12.25) and wider dispersion (0.7 vs. 0.5) with his method, much of the discrepancy between what my implementation of his method returns and his published result disappears, a testament to how sensitive space-density analyses can be to the choice of input parameters.

In the end, my implementations of these methods all indicate a significantly higher peak density than that derived by Thé and Staller. Given that the uncertainties with such a small sample size can be significant, their disagreement with Murray and Sanduleak is probably not as great as they believed. That a maximum density occurs at a distance of ~ 20 pc is likely a reflection of the fact that this is the approximate displacement of the Sun above the galactic plane (Reed 2006); Thé and Staller did not remark on this point. The controversy generated by their claim appears to have faded from interest; since Branham's

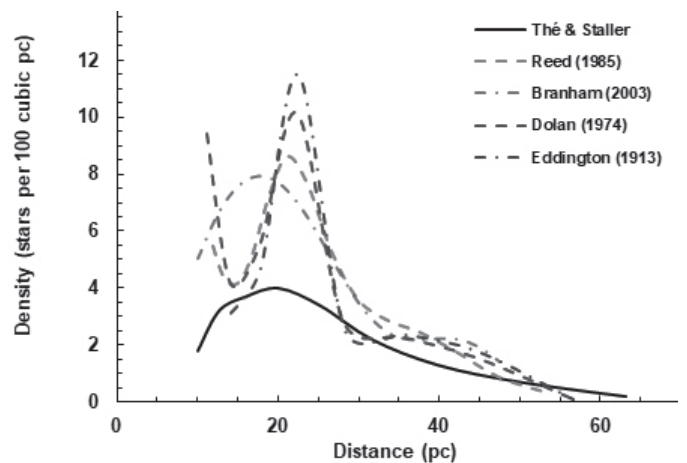


Figure 4 – Results of star-count analyses for south galactic pole M-dwarfs from Thé & Staller (1974).

2003 analysis, their paper has been cited only once, in a paper reporting a survey for new late-type low-mass stars.

6.2 North Galactic Pole K Giants

Uggren (1962) published an extensive analysis of the distribution of a late-type stars in a 396-square-degree region of sky toward

(continued on page 26)



The northern lights are seen here in all their glory at Baptiste Lake in Alberta. The image was taken by the new editor of SkyNews, Allendria Brunjes. She used a Nikon D5200, 18mm, 30 sec, f/3.5, ISO 200.

Klaus Brasch imaged Earthshine from his observatory in Flagstaff, Arizona, with an AP-155 f/7 Starfire EDF refractor and a Canon 6D DSLR last May, though he'd almost forgotten about the images. Exposures were taken at ISO 400, and then stacked and processed in Photoshop CS-6.





The stunning Seven Sisters (M45) was processed by Debra Ceravolo using the Ceravolo 300 Astrograph at $f/4.9$ on an Astrophysics 900 mount. Data was acquired by Peter Ceravolo using an Apogee U16M with Astrodon filters, LRGB 36 one-minute subs for a total exposure of 2.8 hours. All calibration and processing in PixInsight.

Blair Macdonald imaged NGC733, a spiral galaxy about 40 million light-years away. Blair says. "It is the closest member of the Deer Lick Group, an optical grouping of galaxies that are not a true cluster. Instead they are just a chance optical alignment of five galaxies." Stephan's Quintet is also visible in the lower left of the frame. Blair captured the image at the Nova East Star Party of the Halifax Centre of the RASC in September 2019. Total exposure was 70 minutes (14 X 5 minutes) using an Optics Sky-Watcher Esprit 120 $f/7$ APO refractor with a focal length of 840 mm and a Canon 60Da DSLR. Calibration, stacking and masked stretching done with Images Plus.



(continued from page 23)

the north galactic pole. Like the Thé & Staller M-dwarf counts above, this data makes for a convenient test case as the interstellar extinction is minimal and the fictitious densities can be taken to be real densities. In his 2003 paper, Branham analyzed Upgren's counts for K0 giants, presumably a well-defined spectral grouping. Upgren lists "smoothed" counts of stars per 100 square degrees between B magnitudes 5.0 and 13.0 in half-magnitude intervals; for the K0 giants these total 155.6 stars, so there must have been some 620 in reality. Upgren performed a traditional $(m, \log \pi)$ analysis, assuming a Gaussian LF with MO = 1.8 and $\sigma = 0.8$.

I have re-analyzed these data with the Branham, Dolan, and my 1985 methods; the results are shown in Figure 5. (The Eddington method was tried but resulted in wild oscillations at nearby distances and so is not included here.) Beyond about 150 pc, my and Dolan's methods track Upgren's results surprisingly closely, while my implementation of Branham's method yields results of about the same magnitude but with the density declining almost linearly down to zero at about 650 pc. (After this distance the Branham density does go slightly negative, but then recovers to slightly positive numbers beyond about 900 pc; this is not shown in Figure 5.) This again conflicts with what Branham found for this data, and also again we have been unable to pin down the source of this discrepancy. I am confident that my implementation of Branham's method is sound given its solid performance with my simulated data, but in the end remain puzzled at the discrepancies on applying the method to real data. The consistency of results between my method and Dolan's (and, in some cases, Eddington's) is encouraging.

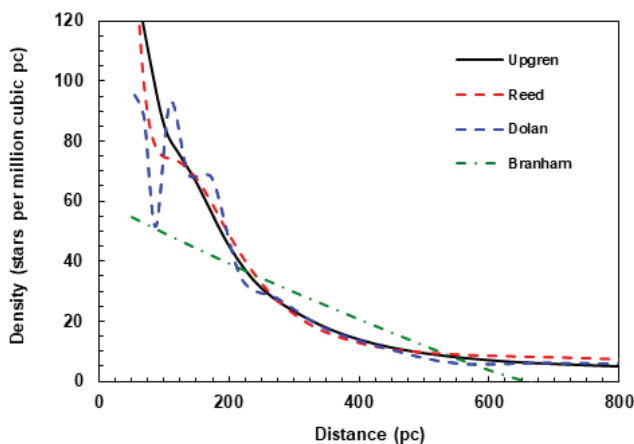


Figure 5 — Results of star-count analyses for north galactic pole K giants from Upgren (1962).

Summary

The main conclusion of this paper is, not surprisingly, that not all methods of analyzing star-count data created equally reliable results. The Eddington (1913), Dolan (1974), Reed (1985), and Branham (2003) algorithms are definitely the front-runners. The Reed and Branham methods are preferable in view of the ease with which they could accommodate different luminosity functions. Branham's method is more mathematically sophisticated so far as deconvolving an inherently ill-posed problem is concerned, but possesses the ambiguity of the choice of the ridge parameter. My 1985 method has the advantages of conceptual simplicity and always generating positive densities, if the initial guess is positive at all distances, although potentially at the cost of being more prone to the front-loading effect.

Most pre-computer-era space-density analyses should probably be regarded with skepticism; an ambitious student of the history of astronomy might wish to compile them all and re-run them in a consistent way using one or more of the methods advocated here. But this is not to say that those studies were meaningless; their fundamental data on thousands of stars are still valid and serve as valuable calibration points for galactic-structure models. Patient human computers were working with the best data, observational technologies, and computational techniques available to them, wringing what they could out of inherently noisy data and no doubt aware of the uncertainties they were up against. In these days when so much data is available at the click of a mouse, we should remember their efforts with respect and humility. ★

Acknowledgements

I am grateful to Richard Branham for discussions on this paper. My interest in star counts goes back to my days as a graduate student in the early 1980s at the University of Waterloo under the mentorship of Dr. Pim FitzGerald, and it is to his lasting good influence that I owe much of my subsequent scientific career.

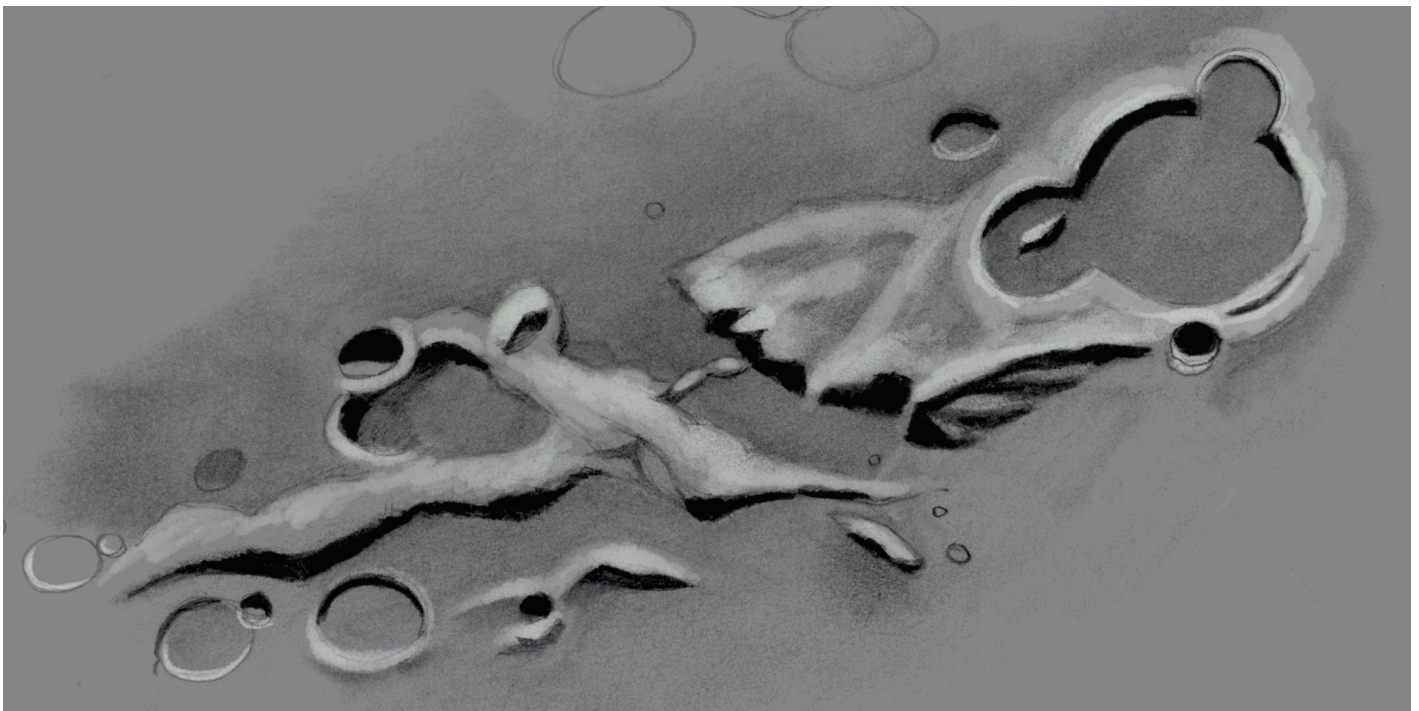
References

- Bahcall, J.N. & Soneira, R.M., 1980. The Universe at Faint Magnitudes. I. Models for the Galaxy and Predicted Star Counts. *ApJ Supplement Series* 44: 73–110. <https://doi.org/10.1086/190685>
- Bahcall, J.N., 1986. Star Counts and Galactic Structure. *Annual Reviews of Astronomy and Astrophysics* 24: 577–611. <https://doi.org/10.1146/annurev.aa.24.090186.003045>
- Bok, B.J., 1937. *The Distribution of the Stars in Space*. Chicago: The University of Chicago Press.

- Branham, R.L., 2003. A method for deriving stellar space densities. *AA* 401: 951–958. <https://doi.org/10.1051/0004-6361:20030152>
- Crowder, H.K., 1959. On the Computation of Stellar Space Density Functions. *AJ* 64: 22–25. <https://doi.org/10.1086/107846>
- Dolan, J.F., 1974. A Matrix Method of deriving Stellar Space Densities. *AA* 35: 105–114.
- Dolan, J.F., 1975. The Space Density of M Dwarfs in the Region of the South Galactic Pole. *AA* 39: 463–464.
- Eddington, A.S., 1913. On a Formula for Correcting Statistics for the effects of a known Probable Error of Observation. *MNRAS* 73: 359–360. <https://doi.org/10.1093/mnras/73.5.359>
- Gschwind, P., 1975. RGU Three Colour Photometry in the Large Sagittarius Cloud. *AA Supplement Series* 19: 281–302.
- Kapteyn, J.C., 1922. First attempt at a theory of the arrangement and motion of the sidereal system. *AJ* 55: 302–327. <https://doi.org/10.1086/142670>
- Lucy, L.B., 1974. An iterative technique for the rectification of observed distributions. *AJ* 79(6): 745–754. <https://doi.org/10.1086/111605>
- McCuskey, S.W., 1965. Distribution of the Common Stars in the Galactic Plane. In: *Galactic Structure*. Chicago: University of Chicago Press.
- McCuskey, S.W., 1983. Space distribution of stars in the Southern Milky Way. III. A region in Centaurus-Crux. *AJ* 88(8): 1175–1181. <https://doi.org/10.1086/113407>
- Mihalas, D. & Routly, P.M., 1968. *Galactic Astronomy*. San Francisco: W.H. Freeman and Company.
- Mihalas, D. & Binney, J., 1981. *Galactic Astronomy: Structure and Kinematics*. San Francisco: W.H. Freeman and Company.
- Murray, C.A. & Sanduleak, N., 1972. Kinematics of faint M stars near the North Galactic Pole, and the Mass Density in the Solar Neighbourhood. *MNRAS* 157: 273–279. <https://doi.org/10.1093/mnras/157.3.273>
- Ochsenbein, F., 1980. A New Method for Deriving Space Densities of Stars. *AA* 86: 321–326.
- Pritchett, C., 1983. Application of star count data to galactic structure. *AJ* 88(10): 1476–88. <https://doi.org/10.1086/113437>
- Reed, B.C., 1983. An analytic solution for stellar space densities. *AA* 118: 229–233.
- Reed, B.C., 1985. An Iterative Solution for Stellar Space Densities. *JRASC* 79: 294–301.
- Reed, B.C., 2006. The Sun's Displacement from the Galactic Plane from Spectroscopic Parallaxes of 2500 OB stars. *JRASC* 100: 146–148.
- Spaenhauer, A.M., 1978. A Systematic Comparison of Four Methods to Derive Stellar Space Densities. *AA* 65: 313–321.
- Thé, P.S. & Staller, R.F.A., 1974. Faint M-Type Stars in the South Galactic Pole Region. *AA* 36: 155–161.
- Trumpler, R.J. & Weaver, H.F., 1953. *Statistical Astronomy*. Los Angeles: University of California Press.
- Uppgren, A.R., 1962. The Space Distribution of Late-Type Stars in a North Galactic Pole Region. *AJ* 67(1) 37–78. <https://doi.org/10.1086/108602>

Great Images

by Michael Gatto



Here's a sketch of Montes Pyrenaeus from 2019 November 2, from Cole Harbour NS. Sketched at the eyepiece for about 90 minutes using a Celestron C102 Achromat and a 13mm Baader Hyperion EP, with tones added later in Procreate. This object is part of the RASC's Explore the Moon observing program.

A Daydream and Poetry among the Stars

by David Levy, Kingston & Montréal Centres

This first installment is a little different. This time I have written a fictitious story about a boy and his dog as they parade about the cosmos, first to the Moon, then to the Dog star. The story is loosely based on a book I wrote when I was in fourth grade. As a child I actually enjoyed a family beagle named Clipper.

Young Stephen was sitting at his desk in school, feeling bored. As he sat, he thought of the beagle, named Clipper, that his parents had bought him.

It was time for Clipper to take young Stephen on a tour through the night sky. On command Clipper appeared and said, “Tonight I will have you meet the Moon and a new star.”

“A brand-new star I have never seen before?” Stephen asked.

“We are going to visit a couple of places in the sky—first the Moon and then the Dog Star.”

“Why?” Stephen asked.

“Because I said so,” Clipper howled. After all, Clipper is a beagle. And beagles are dogs, too.

Suddenly a cloud of whirling gases appeared out of nowhere. As Stephen hugged Clipper tightly, both boy and beagle slipped into a wormhole and somehow navigated through space and time. When they emerged, they were walking on the Moon. All was white, and mountains and crater walls



Figure 2 — The little beagle, Clipper, taken around 1956, probably by the author with a Kodak Brownie Holiday camera.

towered into the sky. Despite this blaze of light, the sky was still studded with stars.

Suddenly a strange creature appeared. It looked like a paper shopping bag. It had four small feet at the bottom, two little arms on top, and a head also on top. Clipper went up and gave the new creature a sniff.

“My name is Tanya,” she said. “I look very strange because I live only on the Moon. I will guard you and Stephen while you are here. When you look at the Moon, or the sky, think of me.”

“I can walk on the Moon,” Stephen muttered to himself as Tanya and the beagle toddled along with him. “Why am I able to do this?”

“Because the Moon is not just an object in the sky,” Tanya explained. “It is a place. Twelve people have already walked on the Moon, and some of them are still alive now. Buzz Aldrin, for example, was part of the very first team to walk on the Moon. He still lives and is in good health.”

Clipper snorted in agreement.

Although there are no roads or sidewalks on the Moon, Stephen had no trouble pacing about, climbing the mountains and blazing a trail within small craters. It was a comfortable



Figure 1 — The Moon and Venus. Credit: David Levy

stroll as he was surrounded by the tall distant peaks. Stephen thought of a song:

“I was strolling on the Moon one day, in the merry, merry month of...”

“DECEMBER!” Clipper howled.

“Doesn’t rhyme with May,” Stephen said.

“Gene Cernan and Jack Schmidt, two astronauts who walked on the Moon just as we are now, sang that song during Apollo 17, in December 1972,” Clipper said. “You weren’t even born then.”

The day was getting was late and the Sun sank low. Even though the lunar day was long—almost two weeks—it went rapidly. It was time to move on. Back in their whirlwind of a spaceship, they bumped about and raced through space and time. In a flash they were at their second stop.

It was the Dog star.

“But there are two stars!” Stephen yelled.

“I can hear you! Don’t shriek!” the beagle shot back. “Yes, there are indeed two stars. The brighter one is Sirius, the Dog star. The tiny one nearby is much smaller and dimmer. It is called The Pup.”

Stephen gazed at the pair with joy. Two distant suns, one circling the other, lit up the sky. It turns out that the bigger of the two stars, formally named Sirius, is the brightest star in the sky.

“Stephen,” the teacher woke Stephen suddenly. “Pay attention in class! I will ask you one more time. What is the closest thing to the Earth in space?”

Stephen snapped to alertness. Where did Clipper run off to, he thought. Clipper? Clipper? Clipper!

“The Moon,” Stephen muttered.

At that moment young Stephen discovered the power of a daydream. Without leaving his desk, the boy took his magic dog

and an imaginary friend on a trip into the cosmos. That’s the teaching power, the awesome magic, of daydreams.

When Poetry Reaches the Stars

Long, long ago, when I was as student at Acadia University in Nova Scotia, we studied the poems of Alfred, Lord Tennyson. The English 360 course was taught by one of my favourite professors, Roger Lewis. Tennyson remains one of the truly great English poets, and even in his lifetime he knew that. In 1850, upon the death of William Wordsworth, he was appointed poet laureate by Queen Victoria. In that same year he published *In Memoriam*, arguably his greatest work.

More than a poet, Tennyson enriched his life with a passionate interest in science, particularly the night sky. Did he own a telescope? He surely did. Although he used it often, particularly from his home on the Isle of Wight, he often enjoyed the use of big refractor telescopes in England. He viewed some of the great comets of his time, like Donati in 1858 and Tebutt in 1861. He also noticed the discovery of Neptune in 1846. Not only was he aware of these developments, but he also incorporated them into one of the greatest poems ever written, the epic called *In Memoriam*.

In Memoriam grew out of Tennyson’s profound loss when his best friend, Arthur Hallam, died suddenly and unexpectedly in 1831. His grief evolved into several quatrains of poetry, then many, and he completed the work in 1850. But this poem is far more than an elegy. He framed it as a massive commentary on the progress of science during his time, particularly with regard to organic evolution and astronomy. From its dramatic opening line “Strong son of God, immortal love,” he delves into what the great telescopes of his time could reveal as “Science reaches forth her arms...and charms her secret from the latest moon.”

Figure 3 — Last April, the author photographed a small piece of Comet Thatcher (C/1861 G1). These fragments encounter the Earth’s orbit annually as the Lyrid meteor shower. Tennyson might have seen this comet, but he certainly saw the next one that appeared as the Great Comet of 1861.



2019.04.23 01:08

Passing over his wonderful praise of Darwin's theory of evolution and natural selection, "And let the ape and tiger die," we encounter the epic's truly powerful ending. To write that it is like a bald eagle about to soar in flight is just insufficient. Like a gigantic *Saturn V* as it roars off its launch complex to the Moon, the last two stanzas germinate, then erupt in a fiery tribute to creation itself.

The poem closes with a return to Hallam: "That friend of mine who lives in God..." Tennyson then specifies God as being immortal and loving; "That God, which ever lives and loves."

And then he defines the Universe as an ordered realm with a specific goal: "One God, one law, one element." In that one line, Tennyson summarizes the purpose of *In Memoriam* as a statement about the interplay between science and religion. Finally, Tennyson predicts a goal for the Universe: "and one far-off divine event."

In Tennyson's time that goal was not understood. But a century later, understanding of Hubble's constant opened the great question as to whether the Universe will end in a "big crunch" in which the Universe is condensed into a single point as it was 13.7 billion years ago. The other possibility is that the Universe will continue to expand forever. It is one of these two

far-off events "To which the whole creation moves." And thus, we reach the close of *In Memoriam* as it moves proudly among the stars:

*That friend of mine, who lives in God,
That God, which ever lives and loves,
One God, one law, one element,
And one far-off divine event,
To which the whole creation moves. ★*

David H. Levy is arguably one of the most enthusiastic and famous amateur astronomers of our time. Although he has never taken a class in astronomy, he has written more than three dozen books, has written for three astronomy magazines, and has appeared on television programs featured on the Discovery and the Science channels. Among David's accomplishments are 23 comet discoveries, the most famous being Shoemaker-Levy 9 that collided with Jupiter in 1994, a few hundred shared asteroid discoveries, an Emmy for the documentary Three Minutes to Impact, five honorary doctorates in science, and a Ph.D. that combines astronomy and English Literature. Currently, he is the editor of the web magazine Sky's Up!, has a monthly column, "Skyward," in the local Vail Voice paper and in other publications. David continues to hunt for comets and asteroids, and he lectures worldwide. David was President of the National Sharing the Sky Foundation, which tries to inspire people young and old to enjoy the night sky.

All-Star Telescope

www.All-StarTelescope.com

FREE SHIPPING
on most items*
*see website for details

NOW AVAILABLE—ONLY FROM ALL-STAR!

"I've just sat through the first lesson, and I ABSOLUTELY LOVE what you've done. The information is clear, practical and very well thought out. Your presentation style is warm and inviting, and the production quality is superb! This is, without question, one of the absolute best (if not the best) photo tutorials I've ever seen."
Angelo Ioanides, *ExtraOrdinary Vision* magazine

Canada's recipient of Celestron's Perspectives on Imaging award
1-866-310-8844
Didsbury, Alberta

Celestron's New CGX Mount

Nightscapes and Time-Lapses
A video tutorial by Alan Dyer
A VIDEO TUTORIAL BY ALAN DYER
Nightscapes and Time-Lapses
FROM FIELD TO PHOTOSHOP

Logos: SUN SOLAR SYSTEMS, PREMIER SELECT CELESTRON DEALER, TeleVue, border, Sky-Watcher

Background photo: Flame Nebula by Ken From of All-Star Telescope

Observing

A Simple Small 'Scope

by Chris Beckett, *Unattached*

There are two big advantages with small optical instruments that cannot be ignored. First, they inherently present the widest possible true fields available, an advantage second only to their portability and, as the saying goes, “the best instrument is the one you’ll use the most.” So, what would the widest and most portable instrument look like? This was my guiding question in a quest to find a telescope that would act as a travel companion, teaching aid, and as a quick grab-and-go scope. Also, in recent years, I’ve taken up sketching and it’s a challenge to draw using handheld binoculars, as one must raise, lower, and manipulate paper and pencils in a choreography that is limited by my coordination in the middle of the night.

“You will find the lower power eyepiece the most satisfactory”
—William Tyler Olcott

A few years ago, I was fortunate to be granted permission to observe among the telescopes on the summit of Haleakala volcano on Maui. While my binoculars provided amazing views for scanning the Eta Carina region, I developed a strong desire for a telescope capable of taking in this bright swath of Milky Way and other objects I observe back home. Upon returning to Canada, a quick Google search landed me on www.alpha-lyrae.co.uk and a detailed review and description of the Takahashi FS60, a 60-mm $f/5.9$ fluorite refractor. I was not unfamiliar with this telescope, but it comes with a stock 1.25-inch focuser, which means the field of view would be matched by my 80-mm F7 triplet, leaving the only advantage to the FS60 its diminutive ~3-lb weight, and in my opinion making binoculars a more suitable, and less costly, travel instrument. However, I learned on the alpha-lyrae site that it was possible to adapt a 2-inch focuser from *Starlight Instruments* to this tiny Tak telescope. A quick calculation revealed that, with my widest-field eyepieces, I could achieve a 7.5-degree field, greater than most binoculars, plus gain the ability to use multiple powers, filters, and more convenient sketching ergonomics. Around this time, other manufacturers brought out 60-mm scopes with 2-inch focusers but my order was placed and these other scopes were not as light, nor did they have the ultimate portability features I’ll get into in more detail below. In fact, I ended up making an extensive comparison when a friend bought the William Optics 60-mm $f/6$ and it proved to have excellent optics but is not much more portable than other small refractors.



Figure 1 — The tiny Takahashi FS60 and an assortment of wide-field eyepieces and all the accessories needed for a night under the stars. Image by the author.

“Every moment spent under a dark starry sky is precious, and that time is limited.”

—Tim Spiegelberg

The FS60 also has a feature that I thought was unique to the Borg telescopes: you can unthread all components to break it up for travel. For air travel, I drop the lens element into a padded camera bag and take it as carry on while the tube and focuser travel wrapped in a sweater in my luggage. It has been a lot of fun bumping into fellow observers in airports and producing the Takahashi fluorite lens when asked about my observing plans! Mounting such a lightweight scope requires some care but a quick call to Universal Astronomics landed a 1-lb alt-az mount at my door and can be mounted on any inexpensive tripod I might be able to buy or borrow where ever I land. All told, the scope, mount, diagonal and eyepieces come in at less than 6 lb, and split between carry on and checked baggage, it’s a barely noticeable addition. In fact, broken up this way it’s easier than caring for binoculars in transit. Additionally, this telescope comes with a 1.7 \times extender, which threads into the tube section creating a second scope configuration for 60-mm $f/10$. If this wasn’t enough, it’s even possible to purchase a thread-on 76-mm lens that



Figure 2 — An example of the astounding field the Tiny Tak takes in using wide-angle 2-inch eyepieces. Image from SkySafari Pro.

do, and since everyone has bigger telescopes, if more aperture is needed, I just bum a view. One limitation is that, in marginal situations where transparency is poor, there just aren't the photons present to see anything. But it is so easy to set up the scope I frequently get up at night when camping and haul it out for views when it clears and setting anything larger up at 3 a.m. feels like a hassle. In fact, the scope nearly has the portability of a small pair of binoculars, but the size and magnification bump brings in more objects. For example, one particularly clear morning I was able to observe the "False Comet," a complex including NGC 6231 in the bottom of Scorpius, from my parents' home in

is also compatible with the extender, providing 4 telescopic configurations! I bought the 1.7× and use this arrangement in the rare events when it clears on the nights I teach my astronomy class and there's something worth looking at from downtown Regina.

"Technique is the heart of using minimal equipment successfully."

—Jay Reynolds Freeman

Oddly, a 60-mm telescope is an advanced piece of equipment since you need to work a little and use your skills more than with larger instruments. For example, many fainter objects remain invisible to those unaccustomed to small-scope observing. Yet it is an incredibly fun telescope to use. My observing friends enjoy seeing just what a 60-mm scope can

Nova Scotia, a dark location I often visit but typically only have taken binoculars in the past. In this instance, the complex was invisible with hand-held binoculars while the FS60 has just that much more grasp to see such elusive targets. It is incredible to see the Veil Nebula with all this sky around it, not to mention huge swaths of the Milky Way and entire asterisms, such as the bright stars of Vulpecula, appear all in one eyepiece field! ★

Chris Beckett is a past chair and now a regular member of the Observing Committee, a long-time binocular and small telescope observer and author of the RASC Observer's Handbook WIDE-FIELD WONDERS. Since 2012, he has been the Continuing Education Astronomy Instructor at the University of Regina and enjoys observing under the dark skies of Grasslands National Park in the desert environment of southwestern Saskatchewan.

Binary Universe

Charts of the Sky



by Blake Nancarrow, Toronto Centre
(blaken@computer-ease.com)

Planetaria

Planetarium software displays charts of stars for any date and location. Using a computer allows things beyond atlases or books such as accurately showing positions of Solar System bodies. If using the software at the telescope, you can corroborate what you're seeing.

There are a number of planetarium applications available for computers with the most popular arguably being *Stellarium*. In February 2015, I reviewed that app and encouraged new astronomers to try it. I still use it, but it is becoming a computer resource hog.

A decade ago, I used another planetarium tool, Patrick Chevalley's *Cartes du Ciel* or *Skychart*. It rendered the sky accurately and was relatively easy to use. At the time, it was the only app I had that could rotate the field. I would print charts for star parties showing the moons of Jupiter or Saturn. As you know, I am now a fan of SkyTools.

I thought I'd have a look-see with the announcement of a new version. From www.ap-i.net/skychart/en/start I downloaded the Windows 32-bit release 4.2 and it was like reconnecting with an old friend. *Cartes du Ciel* (CdC) presents an attractive sky chart, supports additional catalogues, its basic controls are easy to use, and it remains completely free. Many new features were added, such as observing lists, SAMP compatibility, and connectivity for ASCOM and INDI devices.

Starting

I downloaded the archive "zip" file and that required manually installing the software. Not a big deal but I was on my own without instructions. One might have to log in as an administrator if playing around with the boot drive on a Windows box. If not computer savvy, I'd recommend getting the automated "setup" installer.

I would think the Mac OS install is straight forward (I'll give that a whirl in a month). The download page reminds Linux users to install an additional package.

On launching the app the first time, you are guided through a brief initialization process. Then the main screen of CdC appears, a colourful sky chart (see Figure 1).

The new version sports a streamlined interface with a menu and two tool bars. The date and time are automatically set so the chart then shows what's visible now. You're good to go.

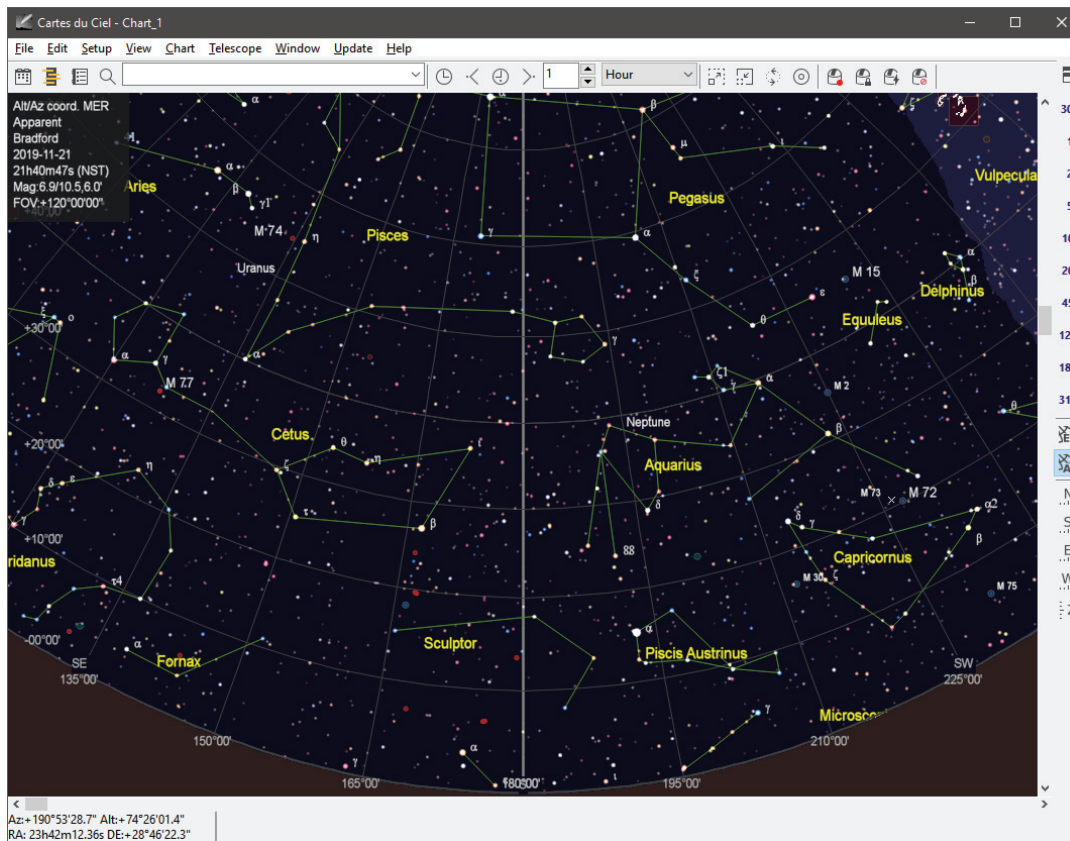


Figure 1 — Main screen on first use. Minimal toolbar mode. Sky chart shows the southern horizon for current date and time.

You can zoom in and out by a variety of methods and pan around with the mouse or keyboard. You can quickly look different directions along the simulated horizon or straight up to zenith.

Finding an object is easy with the search box. Double-click an object for detailed information with links to SIMBAD, Vizier, NED, HyperLEDA, etc.

It's Full of Stars

The "basic" install gives you minimal catalogue data, the software documentation, and many language packs. The basic catalogues provide *HIPPARCOS* stars to magnitude 6.5, Saguro Astronomy Club Deep Sky

Objects, outlines for bright nebulae, and Messier, NGC, and IC objects. For new astronomers with binoculars or a small telescope, or just their eyes, this will be plenty.

I wanted more. I downloaded the “additional stars” indexed package with Tycho-2 stars (about 2.5 million to magnitude 11), the Washington Double Star data, and GCVS variables. This is not for the meek. The files were manually downloaded, decompressed, and put into appropriate folders created in advance. Finally, the catalogues were activated in the Setup menu. Linux users may need root access to install catalogues.

More stars in charts is good for me since, on a clear night from a location free from light pollution, I can tag magnitude 13 to 14 stars in my 8-inch telescope. Like other planetarium apps the display is dynamic, meaning if you zoom out, fainter stars disappear, and when you zoom in to a small field, the limiting magnitude filter shows dimmer objects. I found CdC’s management of stars a little crude. If you’re not satisfied with the steps, you can adjust these Object Filter controls. Also, labels can be disabled, reconfigured, and edited.

I noticed something strange: radial lines around stars. It took me a while to understand this is a normal feature of *Cartes du Ciel*. The lines indicate the separation and position angle to all double-star companions. I could not turn off these distracting lines.

I didn’t dare download the second release of the *Gaia* dataset, which is over 40 gigabytes in size. This may be further complicated by an alternate compression method.

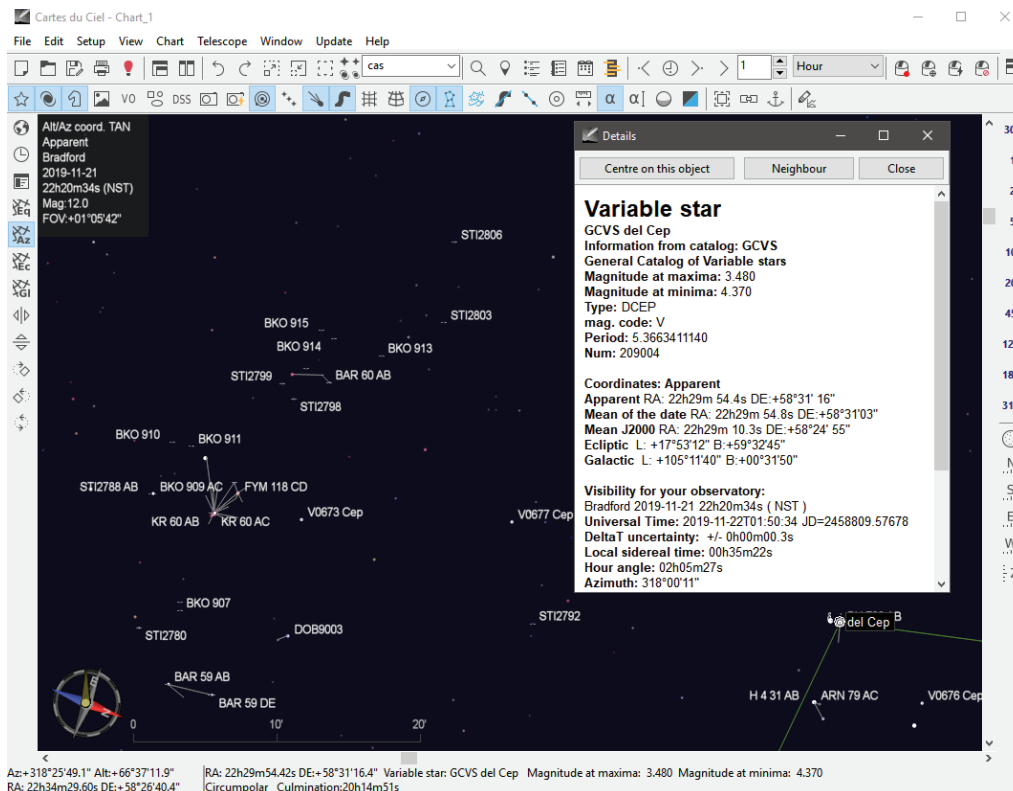


Figure 2 — Standard toolbar configuration. Additional stars showing along with compass rose. Selected object details.

It is relatively easy to update comet and asteroid data by loading from official sources. I did not see an option for novae or supernovae.

Plethora of Display Options

CdC offers many controls for the interface and sky charts.

I prefer more buttons, so I headed to the Toolbar Editor dialogue box to activate the Standard set. This changes the Main bar and turns on the very useful Object and Left bars.

Now it was easy to print, activate red-light mode, toggle on or off nebula outlines, digital images, the ecliptic line, the planets, asteroids, comets, the Milky Way shading, gridlines, constellation lines or borders, the ground, compass rose and scale ruler, and so on.

You can quickly show more or fewer stars or deep-sky objects with the toolbar button. This takes a little getting used to as each corner of the button is sensitive.

I like the comet display in CdC. It’s one of the most realistic I’ve seen with a circular gradient around the comet’s coma with diffuse fanning-out tail. The colour seems too blue, but you can change that.

When you want to fine-tune, you’ll need to make some trips into the extensive Setup menu. Ultimately you can change just about everything. I like the “Apply” button—it lets you try things first.

I was a little irked that red mode only changes the window content. The chrome around the application, the toolbars, and a few other elements do not dim. In Windows you might use a general-purpose app (e.g. Backyard Red).

While *Cartes du Ciel* does not try to create photorealistic views like *Stellarium*, you can enable full-screen mode and then turn off the chrome elements for an eerie display. Be careful turning off the menu; you’ll need to know the keyboard shortcut to get it back!

One can quickly grab chart snapshots for articles or slide images. A chart with legend and informative header and footer is easily printed in colour.

Framing

The “standard” Left bar allows you to change the chart orientation, e.g. azimuthal or equatorial. There are horizontal and vertical flip and rotate buttons for observers with a mirror diagonal or moveable camera.

CdC allows you to create field-of-view circles (Figure 3) or rectangles, 12 of each. Built-in calculators will crunch some of the numbers for you.

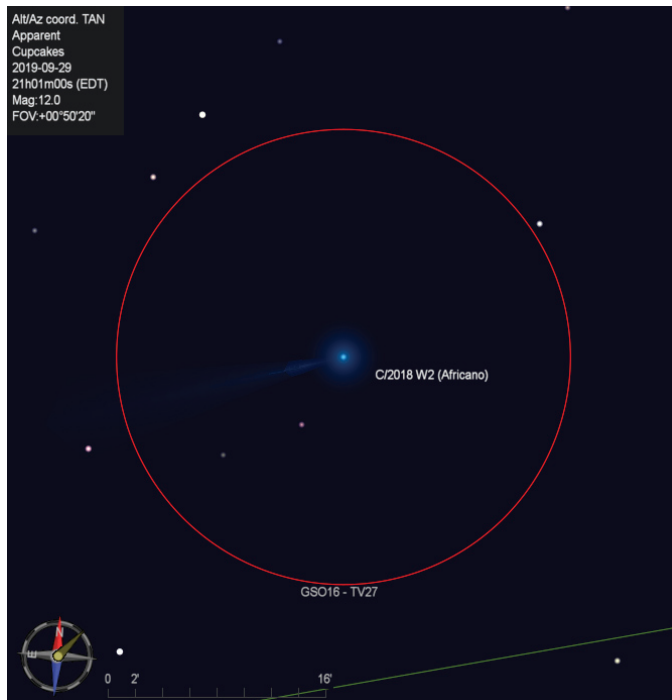


Figure 3 — Screen snapshot of a comet showing the field-of-view circle for the telescope eyepiece.

An interesting feature of CdC is the ability to open as many chart windows as you want. They can be synced to each other or set to show different objects. I'm used to *SkyTools* offering two charts, a wide field atlas, and simulated eyepiece or camera view. Easily done with linking in CdC. In *SkyTools*, if I want to view the whole sky chart for a moment, it closes and resets my other chart windows; not an issue in CdC. You'll need a big monitor for more than a couple charts.

Wait, There's More!

CdC is multi-faceted!

There's a very good Advanced Search feature with controls for finding deep-sky objects, comets, and minor planets (asteroids). Surprisingly it doesn't support Greek letters.

It offers an ephemeris calendar. Tucked away is a twilight times table and eclipse calculator. If I remember correctly, CdC was one of the first planetarium apps I used that had an angular measurement tool.

The app handles Jovian moon shadows but not eclipses.

It offers a number of charts and displays for Solar System objects. I like the table showing planet visibility bars along with the currently selected object.

CdC can automatically load an image of the Sun to show sunspots (if any).

I like the Solar System object plotting tracking feature (Figure 4). I remember calculating trajectories for Uranus and Neptune years ago. Most impressive back then, and still today, is that you can create little videos to dynamically show planetary motion.



Figure 4 — Screen snapshot of plotted path of Uranus. Two months of data shown with annotations every seven days.

There are clever horizon controls. You can load a panoramic photograph to be used for your horizon.

There is a rather amazing variable-star component in CdC. It can automatically generate a list of targets, show light curves, give access to comparison charts, and make it easy to submit observations!

CdC can help you plan and shoot mosaics of large extended objects.

The app accommodates for, and can visually show, proper motion.

Clearly *Cartes du Ciel* is quite rich. If you're just starting out that might be a little overwhelming but with some practice in the app you might have everything you need in one piece of software.

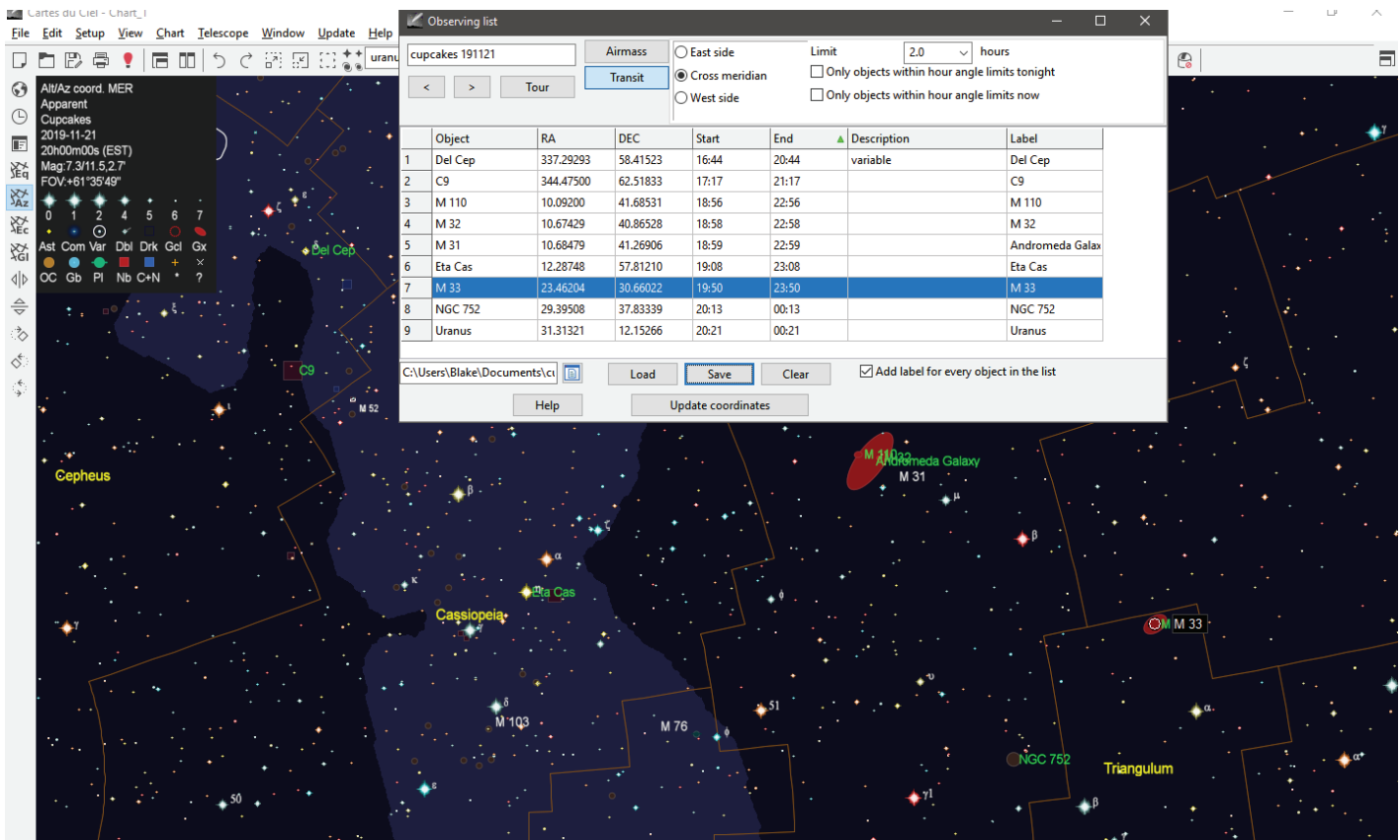


Figure 5 — Observing list with planned targets overtop sky chart with legend. Green text shows target objects.

Looking Ahead

It seems that all planetarium apps now have planning features. You can create and store lists for things you want to look at. This is handy but nothing like full-blown planning apps like *SkyTools* (April 2015), *AstroPlanner* (October 2016), et al.

CdC lets you build and save a planning Observing List (Figure 5). It is easy to add a sky chart target by right-clicking and a very recent update to the app allows adding from the Object List screen! The list is sortable and you can apply filters for hour angle and airmass. The East, Cross, and West times provide important information for visual or photographic projects.

Some users have prepared lists like the Messier and Herschel 400, so you don't have to start from scratch. Adding to the description allows for quick log notes. Items in an active observing list appear with green text in the chart. All that said, CdC can integrate tightly with *AstroPlanner*.

Mount control

Like other apps, CdC allows telescope control. Find an object on the computer screen and slew to it. Easy-peasy!

Using ASCOM mode in CdC, I was able to drive my Vixen Super Polaris mount with GoToStar motors. The Observer

Tools panel (Figure 6) made it easy to move to a selected object, work with targets on a list, pan about, and sync the software and hardware. I understand the latest version of CdC added Park and Unpark commands.

More Info

There is thorough documentation for the *Cartes du Ciel* application, installed locally. There is also lots of information on the website. I noted, however the documentation was edited in April 2017. The 4.2 version has new features not noted. The button symbols changed but the documentation shows the old icons. There's a table of contents but no index. Still, the website offers a search function.

The Quick Start Guide tutorial is good.

There was a vibrant Yahoo!Group; now everything is moved over to Groups.io. The author seems to be active there and on the Cloudy Nights forum.

Summary

Cartes du Ciel is a rich planetarium applicant with good charts, a good interface, and a suite of other useful features. It ran fine on my current and very old Windows computers. It gets five stars out of five from most users. But after all these years, the app is still rough around the edges.

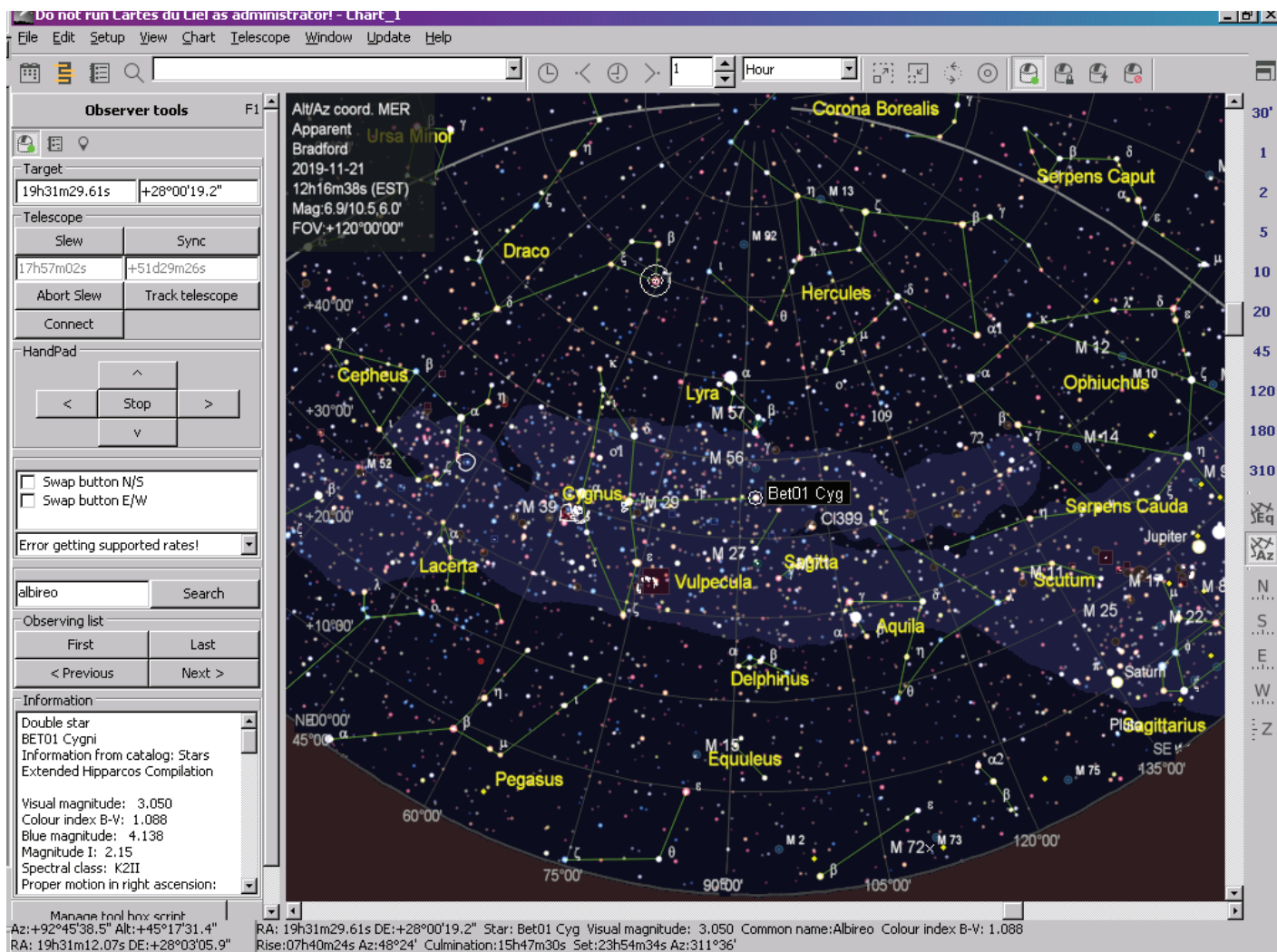


Figure 6 — Toolbox with controls during interactions with telescope mount.

The wording of some things is peculiar, and you may not find some options where you expect. Some of the windows or dialogues are inconsistent in their layout. There's a patchwork feel to the software. While I did not experience anything catastrophic, the app threw error messages that warned of data corruption.

A big worry I have is set-up. I think that installing and configuring the app and, in particular, adding additional catalogues, may present challenges for some.

My biggest concern is old or uncorrected catalogue data. I read a few reports from users about the WDS double-star data being very old. I've come to appreciate all the vetting, sorting, and reconciliation that Greg Crinklaw does with *SkyTools* data. Be wary of errors and omissions in the source data that CdC uses.

You'll often hear the "function versus form" argument when people compare *Cartes du Ciel* and *Stellarium*. Some argue CdC is only for serious astronomers.

You can't beat the price! The developer wants to help you save your money.

Do you want a free planetarium software on your Windows, Mac, and/or Linux machine? Do you want good on-screen or printed charts and basic planning capabilities? Do you like searching for double-star companions or wish to measure variables? Need telescope control? Check out the latest version of *Cartes du Ciel*.

Bits and Bytes

Hot off the press: *SkyTools 4 Visual* is starting beta testing. ★

Blake's interest in astronomy waxed and waned for a number of years but joining the RASC in 2007 changed all that. He supervises at the Toronto Centre Carr Astronomical Observatory, sits on the David Dunlap Observatory committee, helps with volunteer coordination, and is a member of the national Observing Committee. In daylight, Blake works in the IT industry.

Welcome 2020!

by Mary Beth Laychak, Director of Strategic Communications,
Canada-France-Hawaii Telescope

2019 was another excellent year for science at CFHT! Let's take a look back at our 40th-anniversary year and the science highlights it contained. This column borrows liberally from news releases on the CFHT page.

Self-Destructing Asteroid Gault

In January 2019, a team of astronomers from the University of Hawai'i's Asteroid Terrestrial-Impact Last Alert System (ATLAS) used telescopes on Maunaloa and Haleakala to detect the disintegration of asteroid 6447 Gault. A well-known, stable asteroid, Gault's disintegration suggests that asteroids are dynamic, active bodies. Astronomers believe that the subtle, but long-term effects of sunlight can cause asteroids to slowly spin until they begin to crumble, shedding material.

"Each night, the ATLAS survey scans the sky looking for hazardous near-Earth asteroids, and we also observe tens of thousands of known asteroids in the main asteroid belt," said Larry Denneau, ATLAS Project Scientist. "Our collaborator Ken Smith in Belfast found an unusual-looking moving object, and he alerted us that it might be a new comet. Instead, it turned out to be an asteroid in the main belt that just developed a comet-like tail. These events are rare and mysterious, and we were lucky to detect the event right after its turn-on."

Astronomers estimate that this type of event is rare, occurring roughly once a year among the 800,000 known asteroids between Mars and Jupiter. That's why only the latest astronomical surveys—like ATLAS—that map vast swaths of the sky nightly can catch asteroids as they fall apart.

Once the new tail was discovered, Denneau and Institute for Astronomy (IfA) colleague Robert Weryk looked back into archival data from ATLAS and the University of Hawai'i (Panoramic Survey Telescope and Rapid Response System (Pan-STARRS) telescopes. The tail also turned up in data taken as far back as December 2018. In mid-January, a second, shorter tail was spied by Jan Kleyna using the Canada-France-Hawaii Telescope (CFHT), as well as by other observers. An

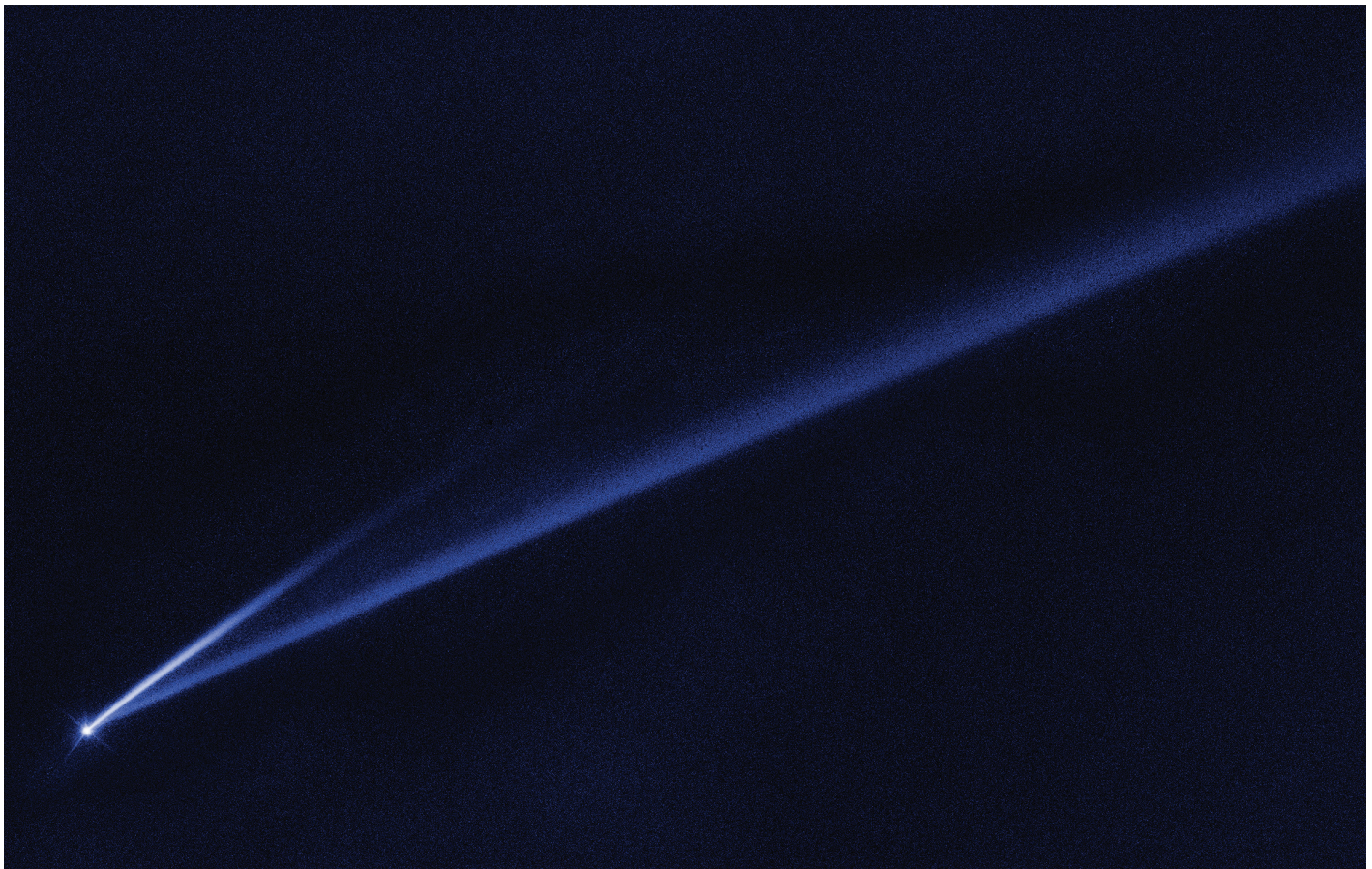


Figure 1 — Hubble Space Telescope captured this striking image of asteroid 6478 Gault, showing two narrow, comet-like tails of dusty debris. Each tail represents an episode in which the asteroid gently shed its material—key evidence that Gault is beginning to come apart. Credit: NASA, ESA, K. Meech, and J. Kleyna (University of Hawai'i), and O. Hainaut (European Southern Observatory).

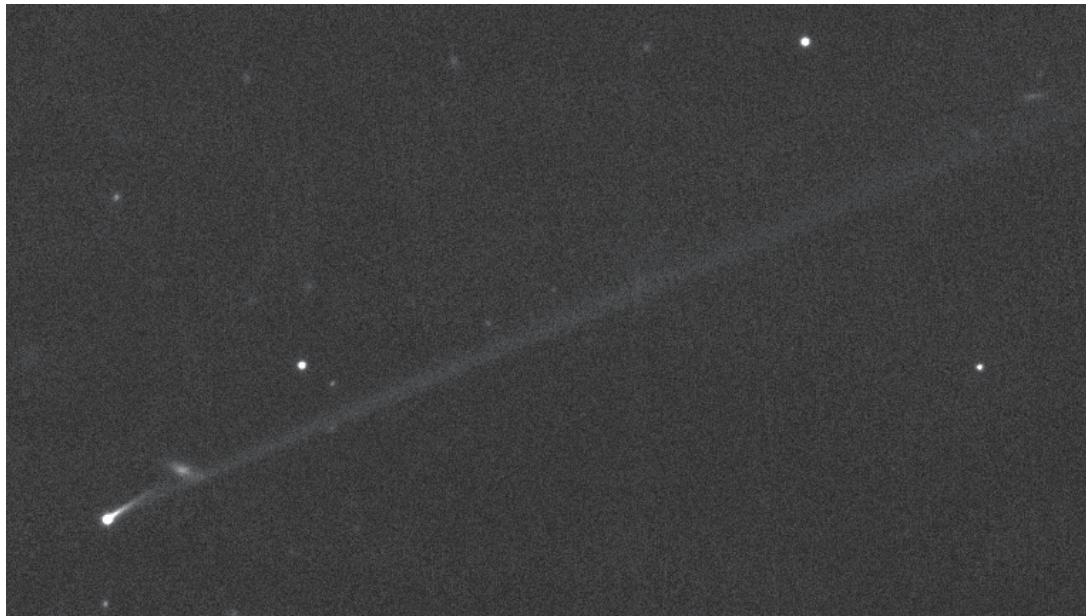


Figure 2 — Asteroid Gault as observed with the Canada-France-Hawaii Telescope on 2019 January 15. Credit: Jan Kleyna (University of Hawai'i), CFHT.

analysis of both tails suggests the two dust releases occurred around 2018 October 28 and December 30.

Tantalized by this new discovery, IfA astronomers, along with colleagues from around the world, began to observe Gault with telescopes on Earth and in space. Spectacular images of asteroid 6478 Gault from NASA/ESA's *Hubble Space Telescope* show two narrow, comet-like tails of debris streaming from the diminutive four-kilometre-wide asteroid. The tails are telltale evidence that Gault is beginning to come apart by gently puffing off material in two separate episodes over the past several months.

Based on observations by the CFHT, the astronomers estimated that the longer tail stretches over half a million miles and is roughly 4,800 kilometres wide. The shorter tail is about a quarter as long.

Added Kleyna: "If the dust cloud lasts a couple of months, and the surveys see things once a month, we will see them. But if traditional observers are looking every couple of years, they'll miss these events."

The researchers hope to monitor Gault for more dust events.

M87 Revealed

One of the keys to CFHT's long-term success has been our large programs. Started in 2003 with the CFHT Legacy Survey, we have continued the tradition with other large programs including VESTIGE, which provided our next science highlight.

VESTIGE, or a Virgo Environmental Survey Tracing Ionized Gas Emission, is one of our current large programs. VESTIGE, led by Alessandro Boselli from Laboratoire d'Astrophysique de Marseille, is using Megacam for 50 nights

from 2017 to 2019. VESTIGE observes the Virgo Cluster in part to learn more about the role of radio monsters and aims to understand the role of environment on galaxy evolution. Using the narrowband H-alpha

filter, the VESTIGE team uses Megacam to conduct a deep imaging survey of the Virgo Cluster. The VESTIGE team recently released an extremely deep image in the narrow-band H-alpha filter of the elliptical galaxy M87. Located at the heart of the Virgo Cluster, M87 is one of the most studied galaxies in the Universe. The image, used on the cover of April's *Astronomy & Astrophysics* journal, reveals the presence of spectacular filaments of ionized gas extending several kiloparsecs from the galaxy. These filaments illustrate an ongoing interaction between M87 and the surrounding environment.

These extremely deep images revealed the presence of spectacular filaments and plumes of ionized gas crossing the galaxy from the southeast to the northwest. Follow-up spectroscopy taken with MUSE at the Very Large Telescope (ESO) suggests that the gas is shock ionized. The geometry of the gas filament and its position in relation to the radio jet and the hot gas previously observed in X-rays suggest that the expanding bubbles ionize the gas. Local instabilities in the intracluster medium cause the gas to cool along magnetically supported filaments into the central elliptical. These filaments may also be the remnant of the cold gas disk of a star-forming galaxy recently accreted by M87 through galactic cannibalism. As the gas falls into galaxy, it may feed the active galactic nucleus (AGN) in the centre of M87 and thus be the origin of the strong radio activity of this intriguing object.

The VESTIGE program is a follow up to a previous CFHT large program, the Next Generation Virgo Survey (NGVS) that observed the same area in the broadband ugriz filters from 2009 to 2012. Over that time, NGVS used the equivalent of ~150 nights to conduct a state-of-the-art optical survey of the Virgo Cluster. The two surveys combined will generate the deepest optical map of the Virgo Cluster ever made.



Figure 3 — The pseudo-colour image of M87 obtained by combining Chandra 1.0-3.5 keV (blue), VESTIGE H-alpha+[NII] (green), and the VLA radio continuum at 90 cm (red) frames of the galaxy. Image credit: VESTIGE team.

The Milky Way's Galactic Cannibalism

A team of researchers from the Strasbourg Astronomical Observatory, Bologna Observatory, and the University of Stockholm has identified a stream of stars that was torn off the globular cluster Omega Centauri. Searching through the 1.7 billion stars observed by the ESA *Gaia* mission, they have identified 309 stars that suggest this globular cluster may actually be the remnant of a dwarf galaxy being torn apart by the gravitational forces of our galaxy.

In 1677, Edmond Halley gave the name “Omega Centauri” (ω Cen) to what he thought was a star in the Centaurus constellation. We now know that Omega Centauri is the most massive globular cluster in the Milky Way: it is about 18,000 light-years from us and contains several million stars that are about 12 billion years old. The nature of this object has been the subject of much debate: is it really a globular cluster, or could it be the heart of a dwarf galaxy whose periphery has been dispersed by the Milky Way?

This dwarf galaxy hypothesis is based on unique features found in ω Cen and not other globular clusters. It contains several stellar populations, with a large range of metallicities that betray a formation over an extended period of time. Most other globular clusters are composed of a seemingly single generation of low metallicity stars, implying they all formed at roughly the same time from the same molecular cloud. If ω Cen is a tidally disrupted dwarf galaxy, astronomers would expect to find debris from the cluster scattered along its orbit in the Milky Way.

Astronomers see evidence of galactic cannibalism around our Milky Way in streams of stars torn off by gravitational tidal forces orbiting the Milky Way. These stars remain visible for a time as stellar streams before becoming dispersed in the vast volumes of interstellar space surrounding the massive galaxy.

By analyzing the motions of stars measured by the *Gaia* satellite with an algorithm called STREAMFINDER developed by the team, the researchers identified several star streams. One of them, named “Fimbulthul” (after one of the rivers in Norse mythology that existed at the beginning of the world), contains 309 stars stretching over 18° in the sky.

The team modelled trajectories of the stars and showed that the Fimbulthul structure is a stellar tidal stream torn off ω Cen extending up to 28° from the cluster. Spectroscopic observations of five stars of this stream with the CFHT show that their velocities are very similar, and that they have metallicities comparable to the stars of ω Cen itself, which reinforces the idea that the tidal stream is linked to ω Cen.

The researchers were then able to show that the stream is also present in the very crowded area of sky in the immediate vicinity of the cluster. Further modelling of the tidal stream will constrain the dynamical history of the dwarf galaxy that was the progenitor of ω Cen, and allow us to find even more stars lost by this system into the halo of the Milky Way. “We are cosmic archaeologists, except we are digging through the fossils of long-dead galaxies rather than human history,” said Professor Lewis, who is a leading member of the survey.

Our December column recapped three more science stories—results from Rosemary Pike and the OSSOS team, new results on the shape of ‘Oumuamau, and Andromeda’s cannibalistic nature. We look forward to bringing new science and new stories from Hawaii in 2020! ★

Mary Beth Laychak has loved astronomy and space since following the missions of Star Trek’s Enterprise. She is the Canada–France–Hawaii Telescope Director of Strategic Communications; the CFHT is located on the summit of Maunakea on the Big Island of Hawaii.

Dish on the Cosmos

Chasing the Origins of Galactic Magnetic Fields



by Erik Rosolowsky, University of Alberta
(rosolowsky@ualberta.ca)

The shape of an object in space can tell you a lot about its nature. Stars and planets are round, which tells us that gravitation is important. Galaxies and planetary systems are shaped like disks, which indicate that their spins govern their shapes. Sometimes the shapes of objects point to more complicated physics, like the spiral arms of a galaxy or the recently observed twisting ropes of radio emission coming from the nearby “Whale” Galaxy (NGC 4631) shown in Figure 1. This radio emission was recently observed by the Very Large Array, a set of telescopes in New Mexico, and the new data yield insights into where galaxies get their magnetic fields.

Magnetism plays a surprisingly important role in shaping galaxies. This may seem natural, since the electromagnetic forces are so much stronger than gravitation. However, the Universe is close to electrically neutral. Since positive and negative charges attract each other, any exposed charge will pull the opposite charge toward it, balancing out the charge. If the flow of charges is continuous, then material can be overall electrically neutral, but the moving charges can create a magnetic field, forming a giant electromagnet in the sky. Because material is constantly moving through the galaxy, these flows generate electric currents and the currents create magnetic fields. These magnetic fields can be strong enough to change the flow of gas in galaxies, even guiding the jets coming from them from forming stars or black holes.

Like the gravitational field, we cannot directly perceive magnetic fields. Instead, we can only see the effects of magnetism, where the main effect is on the polarization of light. Light is an electromagnetic wave, consisting of changing electric and magnetic fields that feed off each other, driving the wave forward. We describe the polarization of the wave in terms of the direction of its electric field. Most physical processes generate light that has its electric field oriented randomly, but when light is generated around magnetic fields, the field gives the light a preferred orientation, which we describe in terms of its polarization.

One of the most common types of polarized light is called synchrotron emission. This emission comes from a rare type of electron that is accelerated up to speeds near the speed of light by supernova shock waves. These fast-travelling electrons are members of a family of particles called cosmic rays. When these cosmic-ray electrons encounter a magnetic field, they

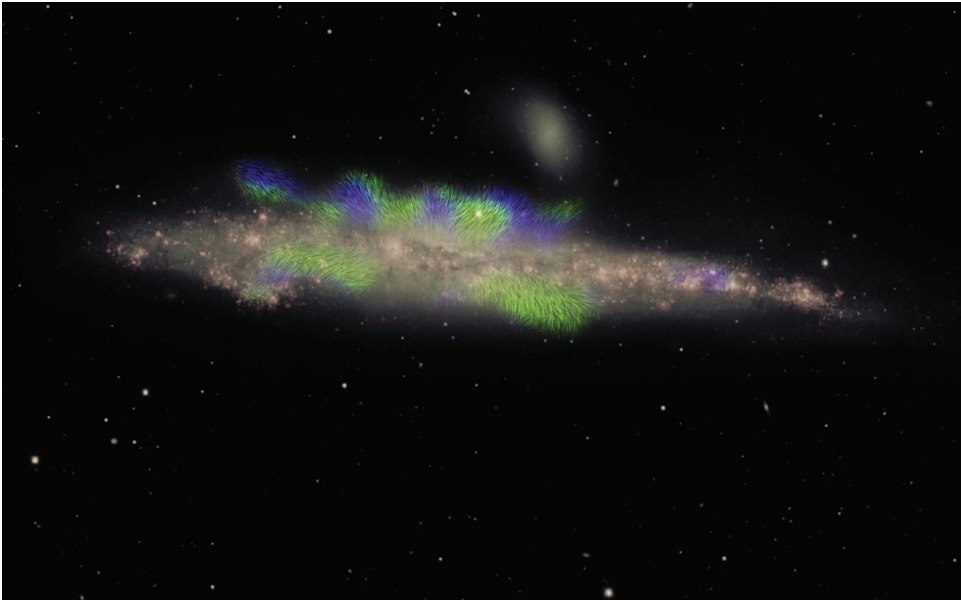


Figure 1 — The Whale Galaxy viewed in optical data with radio emission overlaid as a texture. These new observations reveal organized magnetic fields that extend far above and below the galactic disk. They also find that the magnetic field orientation appears to change direction across the disk of the galaxy.

spiral around it in a helix pattern. The acceleration of the particles generates light that has its polarization set by the orientation of the magnetic field.

This synchrotron emission is what has been observed coming from the Whale Galaxy (Figure 1). The galaxy has been observed edge on and extends above and below the plane of the galaxy in concentrated “ropes” of emission. The polarization of the emission tells astronomers about the orientation of the magnetic field: it points up and out of the disk of the galaxy.

These Very Large Array observations were made by a team of astronomers, led by Prof. Judith Irwin of Queen’s University. Irwin and her team have studied this and several other galaxies, making careful radio observations of the targets to determine the orientation of the field. The goal of this Continuum HALos in Nearby Galaxies—an EVLA Survey (CHANG-ES) is to study the connection between the disks of galaxies and the gas and magnetic fields extended above and below them. The CHANG-ES team has invested years of work to produce the final images shown in the figure, since there can be many sources of artificial polarization signal from the telescope’s electronics.

The novelty of this discovery goes beyond just finding the polarized emission and measuring the orientation of the magnetic field. The CHANG-ES team has also measured the direction of the field, determining where the field points up out of the galaxy, and where it points down into the galaxy. The key insight to making this measurement comes from when some synchrotron emission at the back of the galaxy moves through a region in front of it. As the radio light flows through this region, it encounters other electrons spinning around the magnetic field. Consequently, the polarization is changed by the interaction with the spinning electrons. This “winds” the polarization in a direction that depends on the orientation

of the field. The CHANG-ES team determined which direction the field pointed based on how this winding of the polarization changes across the different frequencies of light observed by the VLA.

The most surprising result of the CHANG-ES study is that the magnetic field appears to reverse

in direction across the disk of the galaxy. In some regions it points out of the disk and in the neighbouring region, it points back into the disk. This “reversal” of the magnetic field goes a long way toward explaining how galaxies generate and sustain their magnetic fields. In particular, this reversing configuration of the field is consistent with generation by a special type of “dynamo.” Dynamos make magnetic fields by driving currents around the disk of a galaxy. The galaxy rotation drives a current that amplifies the galactic magnetic field. The new results of the study show that the field is strong and organized well outside the disk of the galaxy, suggesting that the field is lifted out of the galaxy by winds of material generated by stars.

The careful work on the CHANG-ES team has made great progress in understanding where the elusive magnetic field is being made in galaxies. The quality of the work has been essential for choosing which models of magnetic fields are actually correct. With clearer ideas in place, we can deduce how these fields should change over time and influence the structure of the galaxy. ★

Erik Rosolowsky is a professor of astronomy at the University of Alberta where he researches how star formation influences nearby galaxies. He completes this work using radio and millimetre-wave telescopes, computer simulations, and dangerous amounts of coffee.

Credit: Composite image by Jayanne English of the U. Manitoba, with NRAO VLA radio data from Silvia Carolina Mora-Partiarroyo and Marita Krause of the Max-Planck Institute for Radioastronomy. The observations are part of the project Continuum HALos in Nearby Galaxies – an EVLA Survey (CHANG-ES). The optical data were from the Mayall 4-metre telescope, collected by Maria Patterson and Rene Walterbos of New Mexico State University. Arpad Miskolczi of the U. Bochum provided the software code for tracing the magnetic field lines.

John Percy's Universe

The Scale of the Universe

by John R. Percy
(john.percy@utoronto.ca)

Nothing amazes people, young and old, as much as astronomical scales of size, distance, and time. In this column, we will introduce ways to visualize the scale of distance as we look out into the Universe. Some of these are adaptable for use as classroom or outreach activities. There are lots more on the Internet. Another amazing way to visualize the scale of the Universe is to watch Charles Eames's classic short film *Powers of Ten* on YouTube (1).

The Earth and Moon

This activity fits well with most elementary school science curricula. It deals with the Earth-Moon relationship. Let's represent Earth by a 30-cm (diameter) globe. Then what could represent the Moon, fruit-wise: Blueberry? Grape? Orange? Pumpkin? Let the students think and choose. (An 8-cm orange would be about right.) But how far from Earth should they put it? Let the students work it out and demonstrate it; usually they put it too close. It should be 9 m away—30 Earth diameters. That's on the other side of the classroom!

Earth's atmosphere is about 100 km thick, 1/4000 of the distance to the Moon. How much would that be on your scale model? (About 2 mm.) This helps to visualize and appreciate why the Apollo mission was such an achievement.

The Earth and Sun

The Sun is about 100 times bigger in diameter than Earth. That would be 30 m in the scale model that we just made—large enough to fit in the school gym. And the Sun's distance from Earth is about 100 times its diameter, which is about 3 km. Clearly our model is getting out of hand!

The Spaced-Out Solar System

Thanks to diagrams in books, people have misconceptions about the layout of the Solar System, such as that the planets are relatively close together and evenly spaced and all in a line. Let's switch to a model in which the Sun is a 50-cm beach ball. The distance to Earth is about 100 times this, or 50 m! And Neptune is about 30 times further from the Sun than Earth is, or 1.5 km. In this model, the Solar System would extend throughout our local community. Scale models have been set up in several communities, including downtown Toronto. Perhaps you could design one for your own community! By the way: as the Sun grows old and runs out of

fuel, it will expand and become a red giant, hundreds of times larger than it is now. On our new scale model, the Sun would over-fill the school gym!

There's a popular activity called the pocket Solar System (2) in which students can lay out the planetary distances, to scale, (in a straight line, unfortunately) on a 1-m strip of paper, which they can then fold up and take home.

Interstellar Distances

Now that spacecraft have visited Pluto and beyond, some might think that the nearest star is just another step away. But, in our "beach ball" model, the nearest star to the Sun, Proxima Centauri, would be about 300,000 times further from the Sun than Earth is; it would be in New Zealand!

How Do Astronomers Know?

How do astronomers know the distance to nearby stars such as Proxima Centauri? The answer is parallax. When viewed from two different positions (such as opposite points on Earth's orbit), an object (such as Proxima Centauri) seems to move against the background of more distant stars. Here is a simple activity that you can do to demonstrate this.

Hold your hand at arm's length, with your forefinger (not your middle finger!) pointed upward. Look at your finger with your right eye open, and your left eye closed. Now look at your finger with your right eye closed and your left eye open. What do you observe? Usual answer: "your finger moves." Correct answer: "your finger appears to move." Now move your finger halfway to your nose and repeat the experiment. What do you observe? Your finger appears to move more—twice as much. The parallax effect is inversely proportional to the object's distance.

In the past, astronomers made parallax measurements of stars with ground-based telescopes by observing stars six months apart, when Earth was at opposite points on its orbit. But the parallax is very small—fractions of an angular second of arc—and therefore uncertain. The measurements are now made by spacecraft such as *HIPPARCOS* (1989–1993) and more recently *Gaia* (2013–), which achieve much, much higher accuracy.

There are other methods of determining the distance of stars. Most depend on using parallax and apparent brightness to determine the luminosity or power of certain specific types

The April *Journal* deadline for submissions is 2020 February 1.

See the published schedule at

www.rasc.ca/sites/default/files/jrascschedule2020.pdf



Figure 1 – The Hubble Ultra-Deep Field shows thousands of distant galaxies, up to ten billion light-years away, and seen as they were up to ten billion years ago. Source: NASA/ESA/HST.

of nearby stars—called “standard candles”—and assuming them to have the same luminosity everywhere. If more distant stars of the same type can be identified then, by comparing their apparent brightness with their assumed power, we can calculate their distance by using the inverse-square of brightness: brightness is proportional to luminosity and inversely proportional to the square of the distance. An everyday (or every night) example uses streetlights. We intuitively know the power of a typical streetlight. If we see a distant streetlight at night, we intuitively know how far away it is.

Light-Years and Look-Back Times

We are now dealing with distances that are truly “astronomical.” Kilometres are no longer convenient. So astronomers use

light-years. Yes, light-years are units of distance, not time. A light-year is the distance that light travels in one year, slightly less than ten million million km. Proxima Centauri is about four light-years away. We therefore see it as it was four years ago—the “look-back time.”

Our Milky Way and Its “Local Group”

The Milky Way is the gravitationally bound family of hundreds of billions of stars to which our Sun belongs. It is disk-shaped, about 100,000 light-years in diameter and we are about 25,000 light-years from its centre—out in the suburbs, as it were. Let’s make a model of our Milky Way using a 20-cm-diameter paper plate (or a pair of such paper plates stuck together). You can find another good model at (3). On

our model, the Sun would be about 5 cm from the centre. On this scale, how far would Proxima Centauri be from the Sun? (Answer: a few micrometres; you would need a microscope to see it.)

The Milky Way is densest, star-wise, at the centre or bulge (“downtown Milky Way”). At the very centre or nucleus, there is a super-massive black hole. The stars in the disk orbit the centre in a spiral formation, along with nebulae of gas and dust such as the Orion Nebula. You can decorate your Milky Way model accordingly, if you wish.

But there are limitations to this model. Our Milky Way does not have an abrupt edge like the paper plate does; the density of stars gradually decreases. And the Milky Way is immersed in a halo of invisible “dark matter” whose nature is unknown. The halo is also occupied by about 150 globular star clusters, and individual “free range” stars. Some galaxies are not disk-shaped but are elliptical or spherical. You could use balloons to model these. And galaxies are not all the same size; they range from giants to dwarfs—the most common kind.

Our Milky Way lives in a small group of galaxies, imaginatively called the Local Group. It consists of one other large, disk-shaped galaxy like ours—the Andromeda Galaxy, a.k.a. M31—and dozens of dwarf galaxies. You can model M31 with another paper plate (or two). Since M31 is about 2,000,000 light-years away, and about 100,000 light-years across, its paper plate should be 20 cm in diameter, and about 4 m away. We see M31, not flat-on or edge-on, but tilted. You can incorporate this into your model. And remember that the space around and between the two galaxies is filled with dozens of dwarf galaxies. The Milky Way and M31 are slowly approaching each other and, billions of years from now, will pass through each other, like ghosts in the night.

The Virgo Cluster of Galaxies

The Local Group is situated near the Virgo Cluster of about 1500 galaxies. It is about 60 million light-years away, and about 15 million light-years in diameter. In our model, it would fit in a school gym, 120 m away, on the other side of the school. Imagine such a space, filled with 1500 paper plates (and some balloons) of assorted sizes, and a vast swarm of smaller things, representing all the dwarf galaxies.

Galaxy clusters are the basic building block of the Universe. They are not distributed uniformly through space, however, but are arranged in “filaments” and “voids,” stretching to the edge of the observable Universe. How far away is that? It depends on what we mean by the “edge” of the Universe, and on various cosmological effects such as the accelerating expansion of the Universe, but it is more than 10,000 million light-years—hundreds of times more distant than the centre of the Virgo cluster. In our scale model, vast clusters of 20 cm paper plates, arranged in filaments, would occupy the size of one of the

smaller Great Lakes. The total number would undoubtedly exceed the world’s supply of paper plates.

The Hubble Ultra-Deep Field

Figure 1 shows the Hubble Ultra-Deep Field—one of the most famous images in astronomy. It shows about 10,000 galaxies, in a small area of the sky, imaged over just under a million seconds. Some of the larger, brighter galaxies show spiral form, like the Milky Way. They are the nearer ones: apparent size is proportional to the inverse of the distance; apparent brightness is proportional to the inverse square of the distance. These are two ways in which astronomers measure distances in the Universe—apparent size, and apparent brightness of objects of known size and luminosity.

The smallest, faintest objects in the image are galaxies so distant that their light has taken up to ten billion years to reach us. They are up to ten billion light-years away. We see them as they were, up to ten billion years ago, when they were in their infancy. Astronomers truly have a “time machine” to study how galaxies form and evolve over time! ★

Websites

- 1 www.youtube.com/watch?v=0fKBhvDjuy0
- 2 <https://nightsky.jpl.nasa.gov/docs/SSPocketSS.pdf>
- 3 https://mcdonaldobservatory.org/sites/default/files/pdfs/teachers/build_your_own_galaxy.pdf

John Percy FRASC is Professor Emeritus, Astronomy & Astrophysics and Science Education, University of Toronto, a former President (1978–80) and Honorary President (2013–8) of the RASC.



**Ontario Telescope
and Accessories**

tel. 905-487-6363

Proud seller of iOptron Bresser Explore Scientific Antares Bob's Knobs Lumicon	Your Online source for "GoTo" EQ and Alt/Az mounts Telescopes Finderscopes Camera mounts Mechanical adapters and Accessories
---	--

www.ontariotelescope.com

Ontario Telescope and Accessories, Where OTA means more!

Celestial Events for 2020



by David Garner, Kitchener-Waterloo Centre
(dgarner@celestialreview.space)

The upcoming celestial events for 2020 include solar and lunar eclipses, planetary phenomena, several meteor showers, and a planetary conjunction with Jupiter and Saturn. The following provides a brief overview for you to keep some of the more important events in the back of your mind.

Eclipses

This year the Sun and Moon have some interesting views in store for us, but you may have to travel a fair bit to see these events. On June 21, the day after Summer Solstice, expect an annular solar eclipse. It will be visible from central Africa, northern India, and China. It is scheduled to occur between 4:47 and 8:32 UTC.

Since a solar eclipse always occurs about two weeks before or after a lunar eclipse, then two weeks before the solar eclipse, on the night of June 5 to 6 there will be a penumbral lunar eclipse visible in most of Asia, Australia, Africa, Europe, and parts of South America. Again, two weeks after the solar eclipse there will be another penumbral lunar eclipse on the night of July 4 to 5 that will be visible in North America, South America, and parts of Europe and Africa.

Another solar eclipse is scheduled for December 14, occurring between 14:32 and 17:54 UTC. This time it will be a total solar eclipse and is expected to be visible from Chile and the southern part of South America. The lunar eclipse that occurs two weeks before in this case is again a penumbral lunar eclipse that will occur during the full Moon of November 30. It will be visible from North America, South America, Australia, and much of Asia.

A penumbral lunar eclipse occurs when the Moon passes through the Earth's partial shadow, or penumbra. Unfortunately, penumbral lunar eclipses are difficult to see as the Moon will only be a slight bit darker.

RASC members receiving this *Journal* in electronic format are hereby granted permission to make a single paper copy for their personal use.

For the lunar and planetary enthusiasts, here are some schedules of the Moon and planetary phenomena for 2020:

Moon Phases

Month	New Moon	First Quarter	Full Moon	Last Quarter
January	24	3	10	17
February	23	2	9	15
March	24	2	9	16
April	23	1 and 30	8	14
May	22	30	7	14
June	21	28	5	13
July	20	27	5	13
August	19	25	3	11
September	17	24	2	10
October	16	23	1 and 31	10
November	15	22	30	8
December	14	21	30	8

Planetary Phenomena

Mercury:

Superior Conjunction	Inferior Conjunction	Eastern Elongation	Western Elongation
January 10	February 26	February 10	March 24
May 4	July 1	June 4	July 22
August 17	October 25	October 1	November 10
December 20			

Venus:

Superior Conjunction	Inferior Conjunction	Eastern Elongation	Western Elongation
—	June 3	March 24	August 13

Earth:

Spring Equinox	Summer Solstice	Fall Equinox	Winter Solstice
March 20	June 20	September 22	December 21

Mars:

Opposition	Conjunction	*Stations
October 13	—	Sept. 9 - Nov. 13

Jupiter:

Opposition	Conjunction	*Stations
July 14	—	May 14 – Sept. 12

Saturn:

Opposition	Conjunction	*Stations
July 20	January 13	May 11 – Sept. 29

* Stations refer to the dates when retrograde motion begins and ends.

Uranus:

Opposition	Conjunction
October 31	April 26

Neptune:

Opposition	Conjunction
—	March 8

Meteor Showers:

Quadrantids	January 4
Lyrids	April 22, 23
Eta Aquariids	May 6, 7
Perseids	August 12, 13
Draconids	October 8
Orionids	October 21, 22
Leonids	November 17, 18
Geminids	December 13, 14
Ursids	December 21, 22

Close Encounters: Moon, Jupiter, and Saturn

Since all of the planets lie along the ecliptic, then, as each month of the year progresses, the Moon moves across the sky, close to the ecliptic, and successively passes each of the planets.

One of the more interesting observations of the Moon and planets will be on December 17, when Jupiter and Saturn will be within 1° of each other and both within 3° of the Moon.

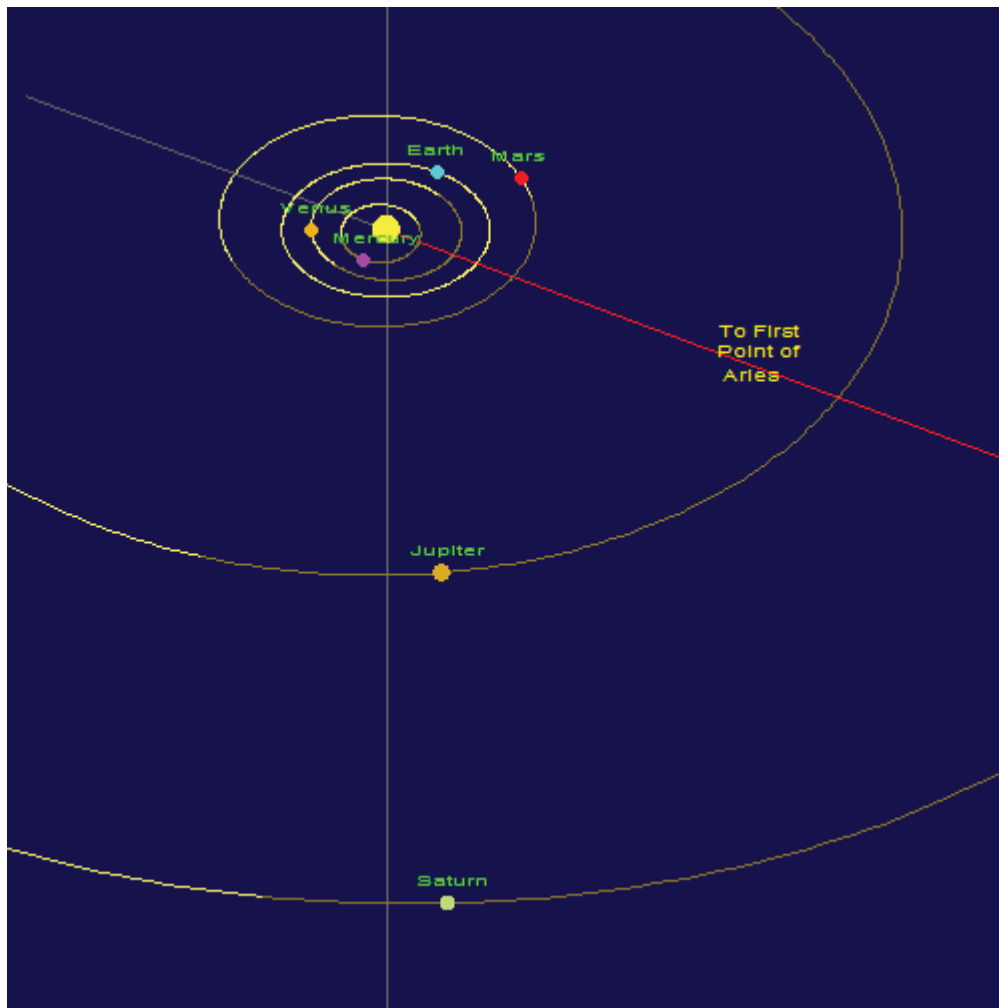


Figure 1 — Jupiter and Saturn in conjunction.

Planetary Alignments

Watch Jupiter and Saturn later this year as they will remain close throughout the months.

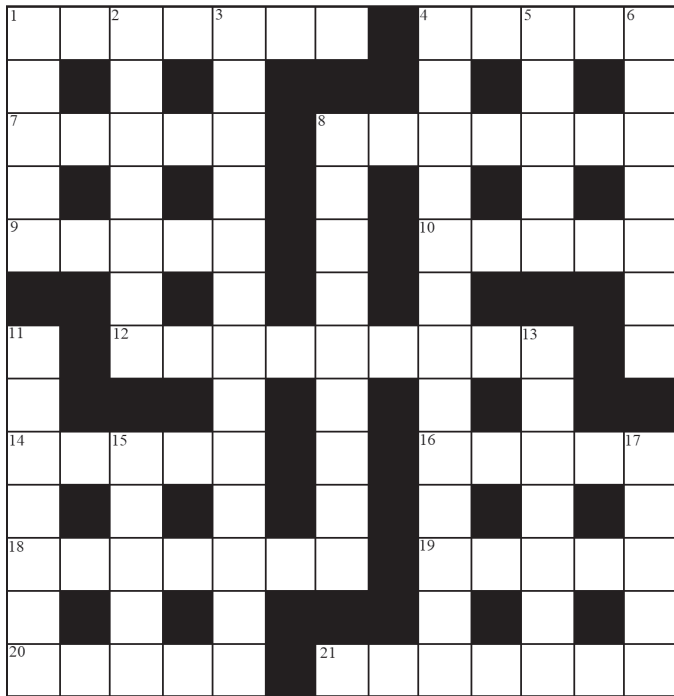
Jupiter and Saturn will finally reach conjunction on December 21, the Winter Solstice, as shown in the figure below, but unfortunately you will only be able to view them for a short time after the Sun sets. Conjunctions between Jupiter and Saturn are not common and interestingly this is their closest conjunction since 1623.

★

Dave Garner teaches astronomy at Conestoga College in Kitchener, Ontario, and is the recipient of the 2017 President's Award. He enjoys observing both deep-sky and Solar System objects, and especially trying to understand their inner workings.

Astrocryptic

by Curt Nason



ACROSS

- Cheer about flopping chub at the Queen's knee (7)
- Flopping frog leads strong Society leader (5)
- Comet discoverer drove a semi in the Governor-General's fleet (5)
- Comet discoverer spun his tire in the bench (7)
- Denebola has an often fatal virus (5)
- Back off nut with hesitation to have it vary frequency (5)
- A number leads a friend to learn how modern music is produced (9)
- Gear parts of a declination drive need brushing (5)
- Bad cuts I get from a shield (5)
- Argon blows around magnifiers (7)
- Operating experience gained about our little fox for plant reproduction (5)
- Misty compiler of impact craters (5)
- Part of the ocular Selene turns about your head (3,4)

DOWN

- The Irish accent did not start with an extragalactic star (5)
- Little credit to one with no identification of a starfish (7)
- Oddly, they grab bingo cards to explain the Universe (3,4,6)
- Step for observing Saturn, but not for all amateurs (2-2,9)
- Alternative charge carrier from a telescope company (5)
- Note a battle is forming in the swan's wing (7)
- Ringo is in Pan's grasp for detecting comets (9)

- Best ESO slides taken around Uranus (7)
- Online outreach source in possible buyout before Easter starts (7)
- Terror doesn't start with a periodic drive correction (5)
- Turn aside your thoughts of improving telescopes (5)

Answers to December's puzzle

ACROSS

1 ARGON (anag); **4** ATTWOOD (anag); **8** RAMSDEN (2 def); **9** INDUS (hid); **10** CREWS (hom); **11** SILICON (anag+LI); **13** NAUGHT (hom); **15** STEREO (anag); **18** BRADLEY (an(D)ag); **19** DRAKE (2 def); **20** OZONE (Oz+one); **22** NEW MOON (anag); **23** NEMESIS (2 def); **24** SAILS (anag)

DOWN

1 AFRICAN (Africano-o); **2** GUM NEBULA (2 def); **3** NODES (anag-i); **4** ALNASL (Al+NASL); **5** TRIPLET (triple+T); **6** OLD (2 def); **7** DYSON (2 def); **12** COR CAROLI (Co+RCA+anag); **14** HALLEYS (H(alley)S); **16** OCEANUS (anag) **17** CYGNUS (Cy+gnus); **18** BROWN (2 def); **19** DAWES (anag); **21** OHM (OH+m)

The Royal Astronomical Society of Canada

Vision

To be Canada's premier organization of amateur and professional astronomers, promoting astronomy to all.

Mission

To enhance understanding of and inspire curiosity about the Universe, through public outreach, education, and support for astronomical research.

Values

- Sharing knowledge and experience
- Collaboration and fellowship
- Enrichment of our community through diversity
- Discovery through the scientific method

THE ROYAL ASTRONOMICAL SOCIETY OF CANADA

Board of Directors and appointed officers for 2020 | Conseil d'administration et membres attitrés pour 2020

Honorary President

Doug Hube, Ph.D., Edmonton

President

Chris Gainor, B.A., M.Sc., Ph.D., Victoria

1st Vice-President

Robyn Foret, Calgary

2nd Vice-President

Charles Ennis, Sunshine Coast

National Secretary

Treasurer

Catherine Carr, B.A. Hon., Toronto

Director and Past President

Colin Haig, B.Sc., M.Sc., Hamilton

Director

Eric Briggs, B.A. Hon., Toronto

Director

Heather Laird, Calgary

Director

Roger Nelson, B.Comm. Hon., Calgary

Executive Director

Philip Groff, B.A. Hon., M.A., Ph.D.

Editors

Journal

Nicole Mortillaro, B.A.A., Toronto

Observer's Handbook

James Edgar, Regina

eBulletin and National Newsletter

Eric Wickham, B.A., Communications and Marketing Coordinator, Mississauga

Observer's Calendar

Paul Gray, Halifax

Great Images

by Nicole Laporte



A beautiful sketch of the Transit of Mercury on 2019 November 11. Nicole Laporte observed the transit from Rigaud, Québec, with a 90mm f/10.1 achromatic Sky-Watcher refractor using a 20mm UW eyepiece and a glass solar filter. "The passing clouds gave the Sun an interesting appearance," she says. The Sun was drawn with a yellow pastel pencil and the clouds with grey chalk, while Mercury was drawn with a fine tip felt pen. "I smudged the pastel colours past the limb of the Sun to capture the clouds that were dimly lit by the Sun," she says.



Journal

Most North Americans don't get to see this beautiful sight, the Small Magellanic Cloud. Michael Watson took the image from Alice Springs, in Australia. He used a Nikon D810a camera body on Tele Vue 127is apochromatic astrograph, mounted on an iOptron CEM40 equatorial mount for a total exposure time of 13 minutes at ISO 5000. Subframes were stacked in RegiStar and processed in Photoshop CS6.